X-900-97-006

MAP Radiation Analysis

J.L. Barth
E.G. Stassinopoulos
G.B. Gee
D.W. Nakamura

August 1997

NASA

National Aeronautics and
Space Administration

Goddard Space Flight Center
Greenbelt, Maryland 20771

MAP RADIATION ANALYSIS

X-900-97-006

J. L. Barth & E. G. Stassinopoulos

Radiation Physics Office
Earth Sciences Directorate
NASA-Goddard Space Flight Center

G. B. Gee and D. W. Nakamura

Systems Engineering and Security, Inc.

August 1997

Goddard Space Flight Center
Greenbelt, MD 20771

Table of Contents

Tables

Figures

MAP RADIATION ANALYSIS

X-900-97-006

J. L. Barth, E. G. Stassinopoulos, G. B. Gee, and D. W. Nakamura

I. Introduction

The purpose of this document is to define the radiation environment in terms of total dose and degradation, single event effects, and displacement damage for the Microwave Anisotropy (MAP) spacecraft. For some electronic components, the total dose values were calculated for specific locations in the spacecraft using a 3-dimensional radiation model of the spacecraft and/or boxes.

The analyses took into account the radiation exposure for both the three month transfer trajectory and the nominal two year mission at the Earth-Sun L2 point. The transfer trajectory was defined by the MAP project office. The results for the transfer trajectory must be used with the understanding that the transfer trajectory may change depending on the launch date.

II. Radiation Effects

Radiation effects that are important to consider for spacecraft design fall roughly into three categories: total dose and degradation effects, single event effects, and displacement damage. Trapped protons, trapped electrons, and solar event protons are primarily responsible for total dose and degradation. As electrons are slowed down, their interactions with orbital electrons of the shielding material produce a secondary photon radiation known as bremsstrahlung. The dose due to galactic cosmic ray ions and proton secondaries is negligible in the presence of the other sources. For surface degradation, it is also important to include the effects of the solar wind plasma.

Single event effects can be caused by heavy ions (solar events and galactic cosmic rays) and protons (trapped and solar events). Displacement damage is primarily due to trapped and solar protons and neutrons that are produced by interactions of primary particles with the atmosphere and spacecraft materials.

III. The MAP Mission

The MAP spacecraft will be transferred out to the L2 point via three phasing loops and a transfer trajectory which are approximately three months in duration. While in the phasing loops, MAP will pass through the trapped proton and electron belts. These exposures could constitute a single event effect risk during some maneuvers but will not contribute to significant dose and degradation or displacement damage. During the transfer trajectory, MAP will also encounter galactic cosmic ray heavy ions and the protons and heavier ions from solar events.

Once MAP is at L2, its mission goal is two years. With the transfer trajectory, the total nominal mission duration is 27 months. With its year 2000 launch date, the entire MAP mission will occur during the maximum phase of the solar cycle which significantly increases the likelihood that the spacecraft will be exposed to particles from solar events (either solar flare or coronal mass ejections). While at L2, the radiation environment encountered by the MAP spacecraft will consist of protons and heavier ions from solar events, galactic cosmic ray heavy ions, and solar wind plasma consisting of low energy protons, electrons, and heavier ions. For the MAP trajectory, the neutron exposure is from secondary neutrons that are produced by primary particle interactions in spacecraft shielding.

IV. Total Dose and Degradation Data

Dose and degradation are cumulative, long term effects. Degradation effects include surface damage, solar cell performance degradation, and detector damage. The total dose accumulation causes performance degradation and failure on memories, power converters, etc.

A. Degradation Environment

The degradation of surface materials is caused by the low energy solar wind plasma. The higher energy particles trapped in the Van Allen belts and from high energy solar events can penetrate solar cell cover glasses and solar array substrate structures and, therefore, are responsible for solar cell degradation.

1. The Plasma Environment

The solar wind is composed of protons and heavier ions (roughly 95% H^+ and 5% He^{++}) combined with enough electrons to form an electrically neutral plasma. It is commonly described in terms of average density, velocity, and temperature. The table below lists average values or a range of values for these parameters.

Average Solar Wind Parameters

Density	1-10 particles/cm^3
Velocity	400 km/s
Energy	"a few eV"

A model of the solar wind plasma that can be used for engineering applications such as material degradation analysis does not exist. However, recent satellite measurements provide a good understanding of the dynamic range of the density, velocity, and energy-temperature.

The plasma environment for the MAP spacecraft will depend on its position relative to the magnetotail region of the earth's magnetosphere*. The data given here from the GEOTAIL and SOHO spacecraft give a sampling of the expected range of the solar wind parameters inside and outside of the magnetotail. The SOHO spacecraft[1] has also measured plasma parameters with the Mass Time-of-Flight/Proton Monitor. Measurements are given here outside of the tail region at ~230 earth radii during January 1997. **Figures 1-3** plot the plasma density, velocity, and energy. A sampling of the data are given in **Table 1**. The data in the table and figures show that the average solar wind parameters compare favorably with the SOHO measurements.

Measurements from the GEOTAIL[2] spacecraft's Comprehensive Plasma Instrument Hot Plasma Analyzer (CPI-HP) were used to determine the dynamic range of the solar wind in the magnetotail region. **Figure 4** shows a segment of the orbit path of the GEOTAIL spacecraft as a function of distance from the Earth in units of earth radii. The trajectory is labeled with Julian days of the year. Note that, at approximately Julian day 310 (in November 1993), the spacecraft was in the magnetotail region near -200 earth radii. At that time, a series of substorms occurred in the tail region. Thus, this sampling should give a good measure of the solar wind parameters to be expected during extreme conditions. **Figures 5-7** plot the plasma density, velocity, and temperature for a 24 hour period during the substorm. A sampling of the data for that time period is given in **Table 2**. The ion composition is roughly 95% H^+ and 5% He^{++}.

A comparison of the SOHO and GEOTAIL measurements for the solar wind shows that the plasma density in the magnetotail can increase to over 100 particles/cm^3 for short periods of time (Figures 1 and 5). Comparing Figures 3 and 7, it can also be seen that the energy of the plasma can increase in the magnetotail from a "few eV" to the keV level. For these samplings, the general description of the velocity as 400 km/s is accurate, however, Figure 6 shows that the solar wind velocity has a large range within a 24-hour period and that the changes are extremely rapid.

2. High Energy Particles - Surface Incident Fluences

The surface incident proton and electron fluences given in this document can be used for solar cell degradation. There are three sources: trapped protons and trapped electrons encountered in the phasing loops and protons from solar events that can occur anytime during the 27-month mission. The proton fluence levels are also used to determine displacement damage effects. All particle fluences are omnidirectional and isotropic.

The trapped particle fluxes are estimated with NASA's AP-8[3] model for protons and AE8[4] model for electrons. The models come in solar minimum and maximum versions. Because the MAP mission is expected to occur entirely during the maximum phase of the

* The magnetotail of the magnetosphere is formed by the interaction of the solar wind with the Earth's magnetic field. In the solar direction, the magnetic field lines are compressed down to ~12 earth radii under average solar-magnetic conditions. In the anti-solar direction, the solar wind "stretches" the magnetic field lines out to hundreds of earth radii, forming the magnetotail.

solar cycle, the solar maximum version was used for these calculations. The uncertainty factors are 2 for the AP-8 and 2 to 5 for the AE-8. These uncertainty factors apply to long term averages expected over a 6 month mission duration. Daily values can fluctuate by 2 to 3 orders of magnitude depending on the level of activity on the sun and within the magnetosphere.

The estimates for solar proton levels are more problematic because there is not a model that includes data from the severe Solar Cycle 22. During that cycle, eight extremely large proton events were measured, with five occurring in a one-year period. Also, the MAP spacecraft will have limited redundancy. Therefore, a conservative approach was used here by applying a 99% confidence level to the existing models.[5,6] The solar proton predictions are not linear over time; therefore, these data may be invalid if extrapolated for longer mission durations.

Total integral fluences as a function of particle energy for the three particles sources are given in **Table 3**. **Figures 8-10** are plots of the energy-fluence spectra for the three particle sources. The energy levels are in units of > MeV and the fluences are in units of particles/cm^2. These values do not include a design margin.

B. Total Dose Calculations

1. Top Level Dose Requirement

For a first approximation, doses are calculated from the surface incident integral fluences as a function of aluminum shield thicknesses for a simple geometry. The geometry model used for spacecraft applications is the solid sphere. The solid sphere doses represent an upper boundary for the dose inside an actual spacecraft. In cases where the amount of shielding surrounding a sensitive location is difficult to estimate, a more detailed analysis of the geometry of the spacecraft structure may be necessary to evaluate the expected dose levels. This is done by modeling the electronic boxes or instruments and the spacecraft structure. The amount of shielding surrounding selected sensitive locations is estimated using solid angle sectoring and 3-dimensional ray tracing. Doses obtained by sectoring methods must be verified for 5-10% of the sensitive locations with full Monte Carlo simulations of particle tracks through the structure for many histories.

Table 4 and **Figures 11 and 12** give the top level total dose requirement for the 27-month MAP mission including contributions from the trapped protons and electrons, including their secondary bremsstrahlung photon dose, and the solar event protons. The doses are given as a function of shield thickness in units of krads in silicon. At the request of the project office, these dose estimates are given with a factor of two design margin. For the nominal 100 mils of equivalent aluminum shielding, the dose requirement is 25 krads-si. For the solar proton dose, 4 extremely large events were used for the 27-month mission duration corresponding to a confidence level of 99%.

2. Dose at Specific Spacecraft Locations

In cases where parts cannot meet the top level design requirement and a "harder" part cannot be substituted, it is often beneficial to employ more accurate methods of determining the dose exposure for some spacecraft components to qualify the parts. One such method for calculating total dose, solid angle sectoring/3-dimensional ray tracing, is accomplished in three steps:

1) Model the spacecraft structure:
   - develop a 3-D model of the spacecraft structures and components
   - develop a material library
   - define sensitive locations.
2) Model the radiation environment:
   - define the spacecraft incident radiation environment
   - develop a particle attenuation model using theoretical shielding configurations (similar to dose-depth curves).
3) Obtain results for each sensitive location:
   - divide the structural model into solid angle sectors
   - ray trace through the sectors to calculate the material mass distribution
   - use the ray trace results to calculate total doses from the particle attenuation model.

Once the basic structural model has been defined, total doses can be obtained for any location in the spacecraft in a short time (in comparison to Monte Carlo methods). The value of dose mitigation measures can be accurately evaluated by adding the changes to the model and recalculating the total dose. For spacecraft with strict weight budgets, the 3-D ray trace technique is a valuable tool in assessing the effects of dose reduction measures that aim to minimize the impact on the weight of the spacecraft. Finally, by using the 3-D ray trace method, the total dose design requirement can be defined at a box or instrument level avoiding unnecessary use of expensive or increasingly unavailable radiation hardened parts.

It was decided to develop a 3-D model of the MAP spacecraft to determine the level of dose for the PSE and MAC electronics boxes and the HEMT AMPs. Also, the model was used to do a parametric study of the box wall thickness requirements of the Line Driver boards and the IRU electronics.

a. MAP Attenuation Model

The spacecraft incident radiation environment used in the attenuation model included the trapped protons and electrons and the protons from solar events predicted for the MAP trajectory (see Table 1). These particles were attenuated through idealized shielding geometries to produce several particle attenuation profiles. Unfortunately, there is not a combination of geometries that represents a best profile fit for all of the particle types. The geometries used in the final attenuation model were chosen based on comparisons between the ray trace results and the results of full Monte Carlo runs for 5 to 10% of the sensitive locations. The goal is to minimize the effect of any profile inaccuracies on the total dose, i.e., the best profile fit is chosen for the highest contributors to the total dose.

b. MAP Structural Model

The structural model includes two components: the library containing the physical structures of the satellite and the material library. As detail is added to the structural model, the total dose values for sensitive locations near the added mass are reduced. The amount of reduction in the total dose depends on the amount of mass already represented in the model.

1. Physical Structure of Satellite: Line drawings were used to evaluate the shielding potential of spacecraft structures. The selected components were converted to a three-dimensional model by representing each structure with shielding potential as one or more solid geometry entities. Structures with uneven mass distribution are modeled conservatively.

The amount of detail incorporated into the satellite model depends upon the shielding potential of the components, the development phase that the flight project is in, and the amount of detail necessary for an accurate analysis of the response at the sensitive location. Also, it is sometimes necessary to add details (e.g., connectors, struts) to verify the relative positions of important structures. The detail in the final 3-D model can vary from empty electronics boxes in a crude satellite structure to electronic boxes with boards and devices in nearly exact satellite structures.

Since the majority of the MAP spacecraft structure doesn't provide a great deal of protection to the sensitive locations, the spacecraft structure was modeled crudely while the structures around the sensitive locations were modeled with more detail. **Figures 13** and **14** show views of the model for the PSE and MAC boxes both of which were modeled with 50 mil aluminum box walls. The HEMT AMP enclosures are simple 1.3 x. 1.1 x. 0.45 inch box structures with nominal 150 mil wall thickness. **Figure 15** gives views of the spacecraft that shows the location of the most exposed Line Driver board, and **Figure 16** shows the IRU box in the spacecraft.

2. Material Library: It is possible to represent any material of known composition in a 3-D radiation model. For the components that were modeled, the materials are shown in the table below.

Material Library for the MAP Spacecraft

Material	Density(gm/cm^3)	Usage
Aluminum	2.70	Various spacecraft structures
Silicon	2.33	Various spacecraft structures, generic circuit board and parts material
Kevlar	1.00	Special structures
Copper	63.54	Grounding planes, some structure
Plastic	0.90	Board guides
Aluminum (Honeycomb)	0.50	Various spacecraft structures
Gamma-alumina	2.56	Special spacecraft structures
Titanium	4.54	Special structures

c. Verification of Results

The ray trace analyses were completed for each sensitive location in the structural model using 1800 solid angle sectors. Repetitive integrations over the solid angle using Monte Carlo techniques were performed to estimate the precision of the sectoring, i.e., if enough sectors were being used.

Using the particle attenuation information and the results from the ray-tracing analysis, the total dose for a 27-month mission was obtained at each sensitive location. To verify the total dose results, Monte Carlo simulations were performed on at least 10% of the sensitive locations and on some external boxes and internal locations.

d. Results of the Ray Trace Analysis

Unlike the dose values given for the top level design requirement, the doses from the 3-D analyses have not had design margins added to them. Generally, it is recommended that a design margin of two be applied to these data. In cases where parts under test show a larger range in performance, it may be necessary to apply larger margins.

Table 5 gives the doses in units of rads-si to be expected in the PSE box for 30 part locations. Each location is named PSEX_Y, where X is the board number and Y is the location of the part on the board as illustrated in **Figure 17**. The doses range from approximately 2 to 5 krads-si.

Table 6 gives the doses for the MAC box for 45 locations. As with the PSE box the sensitive location is coded with MACX_Y. The MAC box has more sensitive locations because it has 3 more boards than the PSE box. For the MAC box, the doses also range from 1.5 to 5 krads-si.

Table 7 gives the doses for the Line Driver boards, the IRU, and the HEMT AMPs. The IRU doses were calculated at the center of a box of aluminum thicknesses ranging from 25 to 125 mils. The calculated doses range from 5 to 15 krads-si without a design margin.

The same approach was used for the Line Driver boards. The boards were encased in aluminum boxes ranging in thickness from 50 to 200 mils. For the Line Driver cards, the doses without design margins were 6 to 10 krads-si.

Table 5 also gives the predicted doses for the HEMT AMPs. They are in a very exposed location on the MAP instrument, however, with their brass packaging, they are well protected from the radiation environment. For these calculations, Monte Carlo particle tracings were required because the sectoring/ray-trace method can be less accurate when the composition of the surrounding material is dominated by higher atomic weight material. The predicted dose level, without a design margin, is 2.3 krads-si showing the shielding effectiveness of the brass.

V. Single Event Effects Analyses

A. Heavy Ion Induced Single Event Effects

Some electronic devices are susceptible to single event effects (SEEs), e.g., single event upsets, single event latch-up, single event burn-out. Because of their ability to penetrate to the sensitive regions of devices and their ability to ionize materials, heavy ions cause SEEs by the direct deposit of charge. The quantity most frequently used to measure an ion's ability to deposit charge in devices is linear energy transfer (LET). Heavy ion abundances are converted to total LET spectra. Once specific parts are selected for the mission and, if necessary, characterized by laboratory testing, the LET spectra for the heavy ions are integrated with the device characterization to calculate SEE rates. Heavy ion populations that have sufficient numbers to be an SEE hazard are the galactic cosmic rays and those from solar events.

1. Galactic Cosmic Rays

The cosmic ray fluxes for elements hydrogen through uranium were used to calculate daily LET spectra for 100 mils nominal aluminum shielding as given in **Table 8** and **Figure 18**. The range of the cosmic ray abundances are bounded by the extrema of the solar minimum and maximum phases of the solar cycle. For this mission, the predicted values are approximately the average of the solar minimum and maximum values. The new CREME96[7] model was used to obtain the cosmic ray heavy ion abundances. This model has an accuracy of 25-40%.

2. Solar Heavy Ions

The heavy ions from solar flares and coronal mass ejections can also produce single event effects. The solar event fluxes for elements hydrogen through uranium were used to calculate LET fluences for 100 mils nominal aluminum shielding in units of average LET flux per second. The intensity of the fluxes varies over the duration of an event, therefore, values are averaged over the worst week of the solar cycle, the worst day of the solar cycle, and the peak of the 99% worst case solar event (October 1989). **Table 9** and

Figure 19 give the solar heavy ion LET predictions for the MAP mission. The new CREME96 model was also used to calculate the solar heavy ion levels. An uncertainty factor for the solar heavy ion model has not been released.

B. Proton Induced Single Event Effects

In some devices, single event effects are also induced by protons. Protons from the trapped radiation belts and from solar events do not generate sufficient ionization (LET < 1 MeV-cm^2/mg) to produce the critical charge necessary for SEEs to occur in most electronics. More typically, protons cause secondary effects through nuclear interactions, that is, spallation and fractionation products. Because the proton energy is important in the production (and the LET) of the secondary particles that cause the SEEs, device sensitivity to these particles is typically expressed as a function of proton energy rather than LET.

1. Trapped Protons

As seen in Section IV, the transfer trajectory passes through the trapped particle radiation belts which do not pose a total dose hazard if adequate shielding is used to stop the electrons. However, the trapped proton levels are a concern in terms of single event effects. The proton fluxes reach levels that are high enough to induce upsets or latchups. If this were to occur in a critical system during one of the two burns, the mission could be jeopardized.

Figure 20 shows the three phasing loops plotted as a function of latitude and altitude. The location of the burns are indicated by "cross" and "ant" symbols. **Figures 21** through **24** show the proton levels predicted for the four passes through the proton belts as described in the table below.

Description of Transfer Trajectory through Trapped Proton Belts

Figure #	Description of Proton Belt Pass
21	Injection into Loops
22	Apogee to Perigee - Loop 1 with Burn 1
23	Apogee to Perigee - Loop 2
24	Apogee to Perigee - Loop 3 with Burn 2

It can be seen from **Figure 24** that the proton fluxes for energies > 30 MeV before and after Burn 2 are high enough to be a concern for single event effects. Therefore, proton energy spectra were calculated at the peak of the belt passes that occurred before and after the burn. These trapped proton peak fluxes must be included in the single event effects analyses. The proton spectra for a nominal 100 mils aluminum shield thickness are given in **Table 10** and **Figure 25**.

2. Solar Protons

Protons from solar events can also be a single event effects hazard for the MAP spacecraft. These enhanced levels of protons could occur any time during the 27-month MAP mission. As with the solar heavy ion LET, solar proton fluxes are averaged over the worst day, worst week , and the peak of the October 1989 solar event. The proton flux averages for a nominal 100 mils of shielding are given in **Table 11** and are compared to the trapped particle peaks in **Figure 25**. Note that, at the higher energies where nuclear interactions producing the high LET secondary particles are more likely to occur, the trapped proton flux levels are higher than the solar proton levels.

IV. Summary

In the process of developing a radiation management plan for the MAP spacecraft, we have seen the value of applying the newer engineering tools and the need for more accurate models of the radiation environment to evaluate the expected radiation levels. As spacecraft design and material technology become more advanced, the shielding margins that were relied on in the past are disappearing, forcing us to take careful account of realistic shielding structures. This problem is compounded by the use of commercial technologies for space applications. Increasingly, the old visual examination method of adding up 4π shielding structures around a sensitive part is inadequate for setting design requirements.

References

1 F. M. Ipavich *et al.*, (in press JGR 1997), Space Physics Group, University of Maryland, "The Solar Wind Proton Monitor on the SOHO Spacecraft," [WWW Dosument], URL http://umtof.umd.edu/papers/pml.htm

2 L. A. Frank, *et al.*, "The Comprehensive Plasma Instrumentation (CPI) for the GEOTAIL Spacecraft," J. Geomag. Geoelec., Vol. 46, pp. 23-37, 1994.

3 D. M. Sawyer and J. I. Vette, "AP-8 Trapped Proton Environment for Solar Maximum and Solar Minimum," NSSDC/WDC-A-R&S, 76-06, NASA/Goddard Space Flight Center, Greenbelt, MD, December 1976.

4 J. I. Vette, "The AE-8 Trapped Electron Model Environment," NSSDC/WDC-A-R&S 91-24, NASA/Goddard Space Flight Center, Greenbelt, MD, November 1991.

5 E. G. Stassinopoulos, "SOLPRO: A Computer Code to Calculate Probabilistic Energetic Solar Flare Protons," NSSDC 74-11, NASA/Goddard Space Flight Data Center, Greenbelt, MD, April 1975.

6 J. Feynman, T. P. Armstrong. L. Dao-Gibner, and S. Silverman, "New Interplanetary Proton Fluence Model," J. Spacecraft, Vol. 27, No. 24, pp 403-410, July-August 1990.

7 A. J. Tylka, J. H. Adams, Jr., P. R. Boberg, W. F. Dietrich, E. O. Flueckiger, E. L. Petersen, M. A. Shea, D. F. Smart, and E. C. Smith, "CREME96: A Revision of the Cosmic Ray Effects on Micro-Electronics Code,: to be published in IEEE Trans. on Nuc. Sci., December 1997.

SOHO CELIAS Proton Monitor Outside Magnetotail ~230-250 Re

Substorm Conditions

Day	Hour	Density (#/cm^3)	Energy (eV)	Bulk Speed (km/s)
11	2	23.4	6.8	425
11	3	18.5	7.5	441
11	4	13.1	14.7	487
11	5	18.1	15.2	489
11	6	14.7	17.6	500

Relaxed Substorm Conditions (medium density/low bulk velocity)

Day	Hour	Density (#/cm^3)	Energy (eV)	Bulk Speed (km/s)
16	3	8.6	1.9	304
16	4	8.1	2.1	313
16	5	5.8	2.3	319
16	6	3.2	2.8	340
16	7	3.2	3.0	331

Relaxed Substorm Conditions (low density/high velocity)

Day	Hour	Density (#/cm^3)	Energy (eV)	Bulk Speed (km/s)
28	23	3.2	14.7	617
29	0	2.7	14.7	610
29	1	2.5	14.1	602
29	2	2.3	14.7	609
29	3	2.6	14.7	612

Table 1

GEOTAIL Comprehensive Plasma Instrument - Hot Plasma Analyzer
Magnetotail Plasma at ~210 Re During Substorm Conditions November 18, 1993

High Density/Low Bulk Velocity and Thermal Energy

Hour	Min	Sec	Density (#/cm^3)	Energy (eV)	Bulk Speed (km/s)
3	50	12.17	27.7	17.8	261.7
3	51	16.17	28.4	20.6	258.1
3	52	20.17	27.5	15.7	256.0
3	53	24.17	38.1	11.7	256.1
3	54	28.17	45.2	9.4	249.2
3	55	32.17	31.2	13.6	251.3
3	56	36.17	31.7	11.5	256.7
3	57	40.17	28.2	14.2	260.4
3	58	44.17	21.1	22.3	261.2
3	59	48.17	26.7	16.4	256.1
4	0	52.17	39.7	11.0	253.0

Low Density/High Bulk Velocity and Thermal Energy

Hour	Min	Sec	Density (#/cm^3)	Energy (eV)	Bulk Speed (km/s)
5	26	12.17	0.1	562.3	307.3
5	27	16.17	0.2	1043.9	331.3
5	28	20.17	0.2	724.9	276.8
5	29	24.17	0.2	1011.3	193.1
5	30	28.17	0.1	1499.4	175.2
5	31	32.17	0.1	1167.0	349.8
5	32	36.17	0.1	1047.4	519.5
5	33	40.17	0.2	642.5	360.5
5	34	44.17	0.1	848.7	369.8
5	35	48.17	0.1	824.7	534.7
5	36	52.17	0.1	1333.9	258.2

Table 2

MAP Mission Exposure: Trapped particles for Phasing Loops + Solar Protons for All 27 Months

Values Do Not Include Design Margins

Total Number of Trapped Particles Encountered in Phasing Loops
Total Integral Fluences, Solar Maximum
Tau = Total Time in Phasing Loops

Proton Energy >MeV	Proton Fluence $\#/cm^2/tau$	Electron Energy >MeV	Electron Fluence $\#/cm^2/tau$
0.04	2.48E+12	0.04	3.69E+12
0.07	2.08E+12	0.07	2.85E+12
0.10	1.76E+12	0.10	2.27E+12
0.50	3.33E+11	0.20	1.11E+12
1.00	7.99E+10	0.30	5.92E+11
2.00	1.24E+10	0.40	3.52E+11
3.00	5.94E+09	0.50	2.21E+11
4.00	3.35E+09	0.60	1.57E+11
5.00	2.14E+09	0.70	1.14E+11
6.00	1.50E+09	0.80	8.75E+10
8.00	8.86E+08	0.90	7.01E+10
10.00	5.50E+08	1.00	5.64E+10
15.00	2.61E+08	1.25	3.47E+10
20.00	1.37E+08	1.50	2.16E+10
25.00	1.05E+08	1.75	1.36E+10
30.00	8.30E+07	2.00	8.67E+09
35.00	7.41E+07	2.25	5.56E+09
40.00	6.64E+07	2.50	3.59E+09
45.00	5.97E+07	2.75	2.21E+09
50.00	5.39E+07	3.00	1.37E+09
60.00	4.73E+07	3.25	8.30E+08
80.00	3.67E+07	3.50	5.07E+08
100.00	2.86E+07	3.75	2.87E+08
150.00	1.62E+07	4.00	1.64E+08
200.00	9.28E+06	4.50	4.65E+07
250.00	5.66E+06	5.00	1.15E+07
300.00	3.47E+06	5.50	2.57E+06
350.00	2.12E+06	6.00	5.34E+05
400.00	1.30E+06	6.50	9.70E+04
500.00	4.92E+05	7.00	1.17E+04

Total Number of Protons from Solar Events
Total Integral Fluence, Magnetospherically Unattenuated
Tau = 27 Months, Confidence Level = 99%, # of Events = 4

Proton Energy >MeV	Proton Fluence $\#/cm^2/tau$
1.00	6.52E+11
4.00	1.71E+11
10.00	9.00E+10
20.00	4.60E+10
30.00	3.16E+10
40.00	2.17E+10
50.00	1.48E+10
60.00	1.02E+10
70.00	7.00E+09
80.00	4.80E+09
90.00	3.28E+09
100.00	2.25E+09
110.00	1.54E+09
120.00	1.06E+09
130.00	7.24E+08
140.00	4.96E+08
150.00	3.41E+08
160.00	2.34E+08
170.00	1.60E+08
180.00	1.10E+08
190.00	7.56E+07
200.00	5.16E+07

Table 3

Dose at The Center of Solid Aluminum Spheres
MAP: L2 + Phasing Loops, Solar Maximum
Values Include x 2 Design Margin

Aluminum Shield Thickness mils	Solar Protons 27 Months $krads_{si}$	Trapped Protons Phasing Loops $krads_{si}$	Electrons Phasing Loops $krads_{si}$	Bremsstrahlung Phasing Loops $krads_{si}$	Total 27 Months* $krads_{si}$
1.5	1138.00	74.00	278.00	0.01	1490.01
2.9	552.00	23.20	169.20	0.02	744.42
4.4	346.00	12.04	124.20	0.02	482.26
5.8	250.00	7.74	96.80	0.02	354.56
7.3	202.00	5.08	75.80	0.02	282.90
8.7	179.00	3.96	61.20	0.02	244.18
11.7	142.80	2.52	43.00	0.02	188.34
14.6	120.00	1.82	31.60	0.02	153.44
29.2	76.40	0.61	10.90	0.02	87.93
43.7	51.60	0.34	5.62	0.01	57.57
58.3	39.00	0.21	3.46	0.01	42.68
72.9	31.80	0.13	2.28	0.01	34.22
87.5	26.60	0.08	1.53	0.01	28.22
100.0	24.14	0.07	1.12	0.01	25.33
116.7	21.20	0.06	0.73	0.00	21.99
145.8	18.08	0.04	0.36	0.00	18.49
218.7	13.18	0.03	0.06	0.00	13.27
291.6	10.24	0.02	0.01	0.00	10.27
364.5	7.82	0.02	0.00	0.00	7.84
437.4	6.30	0.01	0.00	0.00	6.32
510.4	5.18	0.01	0.00	0.00	5.19
583.3	4.44	0.01	0.00	0.00	4.45
656.2	3.54	0.01	0.00	0.00	3.55
729.1	3.08	0.01	0.00	0.00	3.09
802.0	2.68	0.01	0.00	0.00	2.69
874.9	2.24	0.01	0.00	0.00	2.25
947.8	1.91	0.01	0.00	0.00	1.92
1020.7	1.65	0.01	0.00	0.00	1.66
1093.6	1.45	0.01	0.00	0.00	1.46
1166.5	1.31	0.01	0.00	0.00	1.32
1239.4	1.14	0.01	0.00	0.00	1.15
1312.3	1.00	0.01	0.00	0.00	1.01
1385.2	0.87	0.01	0.00	0.00	0.88
1458.2	0.71	0.01	0.00	0.00	0.71

*Includes Phasing Loops

Table 4

Dose for 27-Month Mission Duration

Values Do Not Include a Design Margin

PSE BOX
With Spacecraft Model rads-Si (Sigma Run)

Detector	#	Trapped Protons	Solar Protons	Photons	Electrons	Total
PSE1_A	1	1.60E+01	4.82E+03	1.04E+00	6.25E+01	4.90E+03
PSE1_B	2	1.72E+01	4.76E+03	1.02E+00	7.30E+01	4.85E+03
PSE1_C	3	1.32E+01	3.96E+03	9.26E-01	4.94E+01	4.02E+03
PSE1_D	4	1.06E+01	3.33E+03	8.43E-01	3.58E+01	3.38E+03
PSE1_E	5	8.93E+00	2.74E+03	7.38E-01	2.59E+01	2.78E+03
PSE3_A	6	1.61E+01	4.45E+03	9.72E-01	6.97E+01	4.54E+03
PSE3_B	7	1.74E+01	4.39E+03	9.52E-01	8.03E+01	4.49E+03
PSE3_C	8	1.36E+01	3.67E+03	8.22E-01	5.48E+01	3.74E+03
PSE3_D	9	9.79E+00	2.84E+03	7.31E-01	3.22E+01	2.88E+03
PSE3_E	10	8.69E+00	2.26E+03	6.18E-01	2.70E+01	2.30E+03
PSE5_A	11	1.72E+01	4.49E+03	9.84E-01	8.01E+01	4.59E+03
PSE5_B	12	1.83E+01	4.43E+03	9.63E-01	8.94E+01	4.54E+03
PSE5_C	13	1.34E+01	3.49E+03	8.01E-01	5.59E+01	3.56E+03
PSE5_D	14	9.69E+00	2.73E+03	7.17E-01	3.35E+01	2.77E+03
PSE5_E	15	8.43E+00	2.13E+03	6.00E-01	2.67E+01	2.17E+03
PSE7_A	16	8.99E+00	3.43E+03	8.60E-01	1.45E+01	3.45E+03
PSE7_B	17	9.12E+00	3.35E+03	8.11E-01	1.74E+01	3.38E+03
PSE7_C	18	8.33E+00	3.00E+03	7.38E-01	1.30E+01	3.02E+03
PSE7_D	19	6.64E+00	2.35E+03	6.52E-01	7.60E+00	2.36E+03
PSE7_E	20	6.02E+00	1.92E+03	5.69E-01	7.15E+00	3.36E+03
PSE10_A	21	1.80E+01	4.64E+03	1.01E+00	8.69E+01	3.11E+03
PSE10_B	22	2.04E+01	4.75E+03	1.02E+00	1.07E+02	2.48E+03
PSE10_C	23	1.53E+01	3.80E+03	8.56E-01	7.08E+01	2.01E+03
PSE10_D	24	1.10E+01	2.97E+03	7.62E-01	4.39E+01	4.70E+03
PSE10_E	25	9.95E+00	2.40E+03	6.41E-01	3.73E+01	4.80E+03
PSE11_A	26	1.83E+01	4.75E+03	1.02E+00	8.79E+01	3.91E+03
PSE11_B	27	2.03E+01	4.89E+03	1.03E+00	1.03E+02	3.09E+03
PSE11_C	28	1.01E+01	3.02E+03	7.47E-01	2.99E+01	2.44E+03
PSE11_D	29	9.48E+00	2.78E+03	7.29E-01	3.00E+01	4.79E+03
PSE11_E	30	7.10E+00	2.11E+03	6.11E-01	1.34E+01	4.91E+03

Dose for 27-Month Mission Duration

Values Do Not Include a Design Margin

MAC BOX
With Spacecraft Model rads-Si (Sigma Run)

Detector	#	Trapped Protons	Solar Protons	Photons	Electrons	Total
MAC1_A	31	1.40E+01	4.54E+03	9.92E-01	4.77E+01	4.60E+03
MAC1_B	32	1.51E+01	4.52E+03	9.79E-01	5.56E+01	4.59E+03
MAC1_C	33	1.12E+01	3.48E+03	8.57E-01	3.75E+01	3.53E+03
MAC1_D	34	9.36E+00	3.09E+03	8.04E-01	2.67E+01	3.13E+03
MAC1_E	35	8.12E+00	2.57E+03	7.13E-01	2.02E+01	2.60E+03
MAC2_A	36	1.28E+01	4.22E+03	9.54E-01	4.21E+01	4.28E+03
MAC2_B	37	1.42E+01	4.29E+03	9.48E-01	5.17E+01	4.36E+03
MAC2_C	38	8.65E+00	2.72E+03	7.15E-01	2.12E+01	2.75E+03
MAC2_D	39	7.83E+00	2.56E+03	6.96E-01	1.67E+01	2.59E+03
MAC2_E	40	6.43E+00	1.94E+03	5.90E-01	9.63E+00	1.96E+03
MAC3_A	41	1.29E+01	4.18E+03	9.52E-01	4.43E+01	4.24E+03
MAC3_B	42	1.43E+01	4.24E+03	9.44E-01	5.33E+01	4.31E+03
MAC3_C	43	8.40E+00	2.60E+03	7.04E-01	2.15E+01	2.63E+03
MAC3_D	44	7.79E+00	2.52E+03	6.92E-01	1.74E+01	2.55E+03
MAC3_E	45	6.27E+00	1.86E+03	5.81E-01	9.70E+00	1.88E+03
MAC4_A	46	1.33E+01	4.19E+03	9.54E-01	4.89E+01	4.25E+03
MAC4_B	47	1.46E+01	4.24E+03	9.44E-01	5.67E+01	4.31E+03
MAC4_C	48	8.20E+00	2.49E+03	6.86E-01	2.15E+01	2.52E+03
MAC4_D	49	7.63E+02	2.43E+03	6.77E-01	1.74E+01	3.21E+03
MAC4_E	50	6.13E+00	1.78E+03	5.69E-01	9.71E+00	1.80E+03
MAC6_A	51	1.47E+01	4.11E+03	9.21E-01	6.29E+01	4.19E+03
MAC6_B	52	1.60E+01	4.14E+03	9.14E-01	7.08E+01	4.23E+03
MAC6_C	53	8.15E+00	2.28E+03	6.39E-01	2.33E+01	2.31E+03
MAC6_D	54	7.68E+00	2.27E+03	6.47E-01	2.03E+01	2.30E+03
MAC6_E	55	5.97E+00	1.64E+03	5.39E-01	1.01E+01	1.66E+03
MAC7_A	56	1.46E+01	3.99E+03	9.48E-01	6.61E+01	4.07E+03
MAC7_B	57	1.59E+01	3.96E+03	9.35E-01	7.47E+01	4.05E+03
MAC7_C	58	7.44E+00	2.02E+03	6.38E-01	2.31E+01	2.05E+03
MAC7_D	59	7.38E+00	2.14E+03	6.53E-01	2.16E+01	2.17E+03
MAC7_E	60	5.48E+00	1.47E+03	5.25E-01	1.00E+01	1.49E+03
MAC9_A	61	1.36E+01	4.25E+03	9.74E-01	5.13E+01	4.32E+03
MAC9_B	62	1.54E+01	4.34E+03	9.72E-01	6.39E+01	4.42E+03
MAC9_C	63	1.08E+01	3.14E+03	7.69E-01	3.63E+01	3.19E+03
MAC9_D	64	8.50E+00	2.66E+03	7.18E-01	2.33E+01	2.69E+03
MAC9_E	65	7.36E+00	2.06E+03	6.02E-01	1.73E+01	2.09E+03
MAC10_A	66	1.36E+01	4.30E+03	9.75E-01	5.06E+01	4.37E+03
MAC10_B	67	1.56E+01	4.44E+03	9.78E-01	6.32E+01	4.52E+03
MAC10_C	68	8.75E+00	2.79E+03	7.33E-01	2.22E+01	2.82E+03
MAC10_D	69	8.07E+00	2.61E+03	7.10E-01	1.96E+01	2.64E+03
MAC10_E	70	6.41E+00	1.95E+03	5.97E-01	9.81E+00	1.97E+03
MAC11_A	71	1.58E+01	4.53E+03	9.92E-01	6.69E+01	4.61E+03
MAC11_B	72	1.75E+01	4.65E+03	9.99E-01	7.87E+01	4.75E+03
MAC11_C	73	9.33E+00	2.97E+03	7.51E-01	2.39E+01	3.00E+03
MAC11_D	74	8.63E+00	2.71E+03	7.26E-01	2.31E+01	2.74E+03
MAC11_E	75	6.70E+00	2.07E+03	6.12E-01	1.03E+01	2.09E+03

Table 6

Dose for 27-Month Mission Duration

Values Do Not Include a Design Margin

IRU Box
With Spacecraft Model rads-Si (Sigma Run)

Aluminum Shielding (mils)	Trapped Protons	Solar Protons	Photons	Electrons	Total
25	9.75E+01	1.36E+04	2.10E+00	7.18E+02	1.44E+04
50	3.85E+01	8.56E+03	1.54E+00	2.13E+02	8.81E+03
75	2.00E+01	6.44E+03	1.26E+00	8.50E+01	6.55E+03
100	1.44E+01	5.39E+03	1.09E+00	3.71E+01	5.44E+03
125	1.17E+01	4.68E+03	9.72E-01	1.67E+01	4.71E+03

Line Driver Boards
Inside Spacecraft Model rads-Si (Sigma Run)

Aluminum Shielding (mils)	Trapped Protons	Solar Protons	Photons	Electrons	Total
50	4.03E+01	9.53E+03	1.94E+00	2.44E+02	9.82E+03
62	3.32E+01	8.55E+03	1.82E+00	1.90E+02	8.78E+03
100	2.56E+01	7.20E+03	1.56E+00	1.33E+02	7.36E+03
150	2.30E+01	6.30E+03	1.38E+00	1.16E+02	6.44E+03
200	2.15E+01	5.61E+03	1.27E+00	1.12E+02	5.74E+03

HEMT AMPs
No Spacecraft Model rads-Si (Monte Carlo Run)

Brass Walls (mils)	Trapped Protons	Solar Protons	Photons	Electrons	Total
150	6.45E+00	2.31E+03	5.30E-01	0.00E+00	2.32E+03

Table 7

Integral LET for Interplanetary GCRs (Z=1-92)
100 mils Aluminum Shielding, CREME96

Values Do Not Include Design Margins

LET MeV*cm/mg	LET Fluence #/sqcm/day Solar Minimum	LET MeV*sqcm/mg	LET Fluence #/sqcm/day Solar Maximum
0.10	2.23E+03	0.10	8.73E+02
0.20	9.84E+02	0.20	3.59E+02
0.30	6.35E+02	0.30	2.32E+02
0.40	4.33E+02	0.40	1.52E+02
0.50	3.42E+02	0.50	1.24E+02
0.60	2.90E+02	0.60	1.10E+02
0.70	2.50E+02	0.70	9.66E+01
0.80	2.23E+02	0.80	8.84E+01
0.90	1.98E+02	0.90	7.94E+01
1.00	1.79E+02	1.00	7.22E+01
2.01	3.39E+01	2.01	5.88E+00
3.02	1.43E+01	3.02	2.03E+00
3.99	7.76E+00	3.99	1.02E+00
5.03	4.59E+00	5.03	5.81E-01
5.99	3.07E+00	5.99	3.80E-01
8.00	1.55E+00	8.00	1.90E-01
10.09	9.00E-01	10.09	1.10E-01
11.07	7.17E-01	11.07	8.75E-02
12.01	5.76E-01	12.01	7.04E-02
13.02	4.67E-01	13.02	5.71E-02
13.96	3.85E-01	13.96	4.72E-02
14.97	3.16E-01	14.97	3.88E-02
16.05	2.61E-01	16.05	3.20E-02
17.00	2.20E-01	17.00	2.71E-02
18.02	1.85E-01	18.02	2.27E-02
19.09	1.54E-01	19.09	1.89E-02
20.00	1.30E-01	20.00	1.60E-02
24.93	4.45E-02	24.93	5.50E-03
30.01	6.27E-04	30.01	8.18E-05
34.90	6.86E-05	34.90	1.06E-05
40.11	4.18E-05	40.11	6.50E-06
45.04	2.83E-05	45.04	4.42E-06
49.99	2.00E-05	49.99	3.13E-06
50.58	1.92E-05	50.58	3.00E-06
55.49	1.34E-05	55.49	2.11E-06
60.19	9.38E-06	60.19	1.49E-06
65.28	6.32E-06	65.28	1.01E-06
69.98	4.40E-06	69.98	7.01E-07
75.02	2.83E-06	75.02	4.52E-07
80.43	1.65E-06	80.43	2.63E-07
85.23	7.71E-07	85.23	1.23E-07
90.32	1.94E-07	90.32	3.10E-08
95.71	2.88E-08	95.71	4.60E-09
100.25	1.19E-08	100.25	1.89E-09
101.42	5.27E-09	101.42	8.41E-10
102.61	2.54E-09	102.61	4.05E-10

Table 8

Integral LET for Interplanetary Solar Particle Events (Z=1-92)
100 mils Aluminum Shielding, CREME96

Values Do Not Include Design Margins

LET MeV*cm²/mg	LET Fluence #/cm²/s Average Over Peak	LET Fluence #/cm²/s Average Over Worst Day	LET Fluence #/cm²/s Average Over Worst Week
0.10	5.16E+02	1.37E+02	2.27E+01
0.20	1.75E+02	4.63E+01	7.53E+00
0.30	7.90E+01	2.09E+01	3.45E+00
0.40	4.36E+01	1.15E+01	1.95E+00
0.50	2.75E+01	7.30E+00	1.26E+00
0.60	1.86E+01	4.94E+00	8.78E-01
0.70	1.35E+01	3.58E+00	6.52E-01
0.81	9.85E+00	2.62E+00	4.91E-01
0.90	7.55E+00	2.02E+00	3.87E-01
1.00	5.88E+00	1.57E+00	3.10E-01
2.01	7.49E-01	2.06E-01	5.99E-02
3.02	4.11E-01	1.13E-01	3.33E-02
3.99	2.64E-01	7.29E-02	2.14E-02
5.03	1.74E-01	4.80E-02	1.42E-02
6.06	1.21E-01	3.36E-02	9.92E-03
7.04	8.68E-02	2.40E-02	7.11E-03
8.00	6.39E-02	1.77E-02	5.26E-03
8.99	5.04E-02	1.40E-02	4.13E-03
10.09	3.85E-02	1.07E-02	3.15E-03
20.00	5.75E-03	1.60E-03	4.63E-04
25.22	2.14E-03	5.95E-04	1.72E-04
30.01	1.83E-05	5.10E-06	1.55E-06
35.30	7.23E-07	2.01E-07	7.14E-08
40.11	3.26E-07	9.08E-08	3.43E-08
45.04	1.95E-07	5.44E-08	2.12E-08
49.99	1.36E-07	3.78E-08	1.48E-08
55.49	8.43E-08	2.35E-08	9.31E-09
60.19	4.92E-08	1.37E-08	5.58E-09
65.28	3.28E-08	9.12E-09	3.75E-09
69.98	2.49E-08	6.92E-09	2.84E-09
75.02	1.80E-08	5.00E-09	2.04E-09
80.43	1.20E-08	3.34E-09	1.36E-09
85.23	6.69E-09	1.86E-09	7.56E-10
90.32	2.03E-09	5.64E-10	2.29E-10
94.61	1.33E-10	3.71E-11	1.51E-11
100.25	5.01E-11	1.39E-11	5.66E-12
101.42	2.22E-11	6.19E-12	2.51E-12
102.61	1.07E-11	2.99E-12	1.21E-12

Peak Differential Proton Fluxes - Phasing Loop Pass #3
100 mils Aluminum Shielding, CREME96
Values Do Not Include Design Margins

Energy MeV	Trapped - Before Burn 2 #/cm^2/s	Energy MeV	Trapped - After Burn 2 #/cm^2/s
0.10	6.58E+01	0.10	4.61E+00
0.13	6.97E+01	0.13	4.89E+00
0.16	7.44E+01	0.16	5.22E+00
0.20	8.02E+01	0.20	5.62E+00
0.25	8.70E+01	0.25	6.09E+00
0.32	9.54E+01	0.32	6.68E+00
0.40	1.06E+02	0.40	7.39E+00
0.50	1.18E+02	0.50	8.24E+00
0.63	1.33E+02	0.63	9.29E+00
0.79	1.51E+02	0.79	1.06E+01
1.00	1.73E+02	1.00	1.21E+01
1.26	2.00E+02	1.26	1.40E+01
1.58	2.33E+02	1.58	1.64E+01
2.00	2.73E+02	2.00	1.92E+01
2.51	3.19E+02	2.51	2.23E+01
3.16	3.71E+02	3.16	2.58E+01
3.98	4.26E+02	3.98	2.95E+01
5.01	4.80E+02	5.01	3.35E+01
6.31	5.25E+02	6.31	3.77E+01
7.94	5.52E+02	7.94	4.24E+01
10.00	5.55E+02	10.00	4.76E+01
12.60	5.32E+02	12.60	5.31E+01
15.80	4.85E+02	15.80	5.84E+01
20.00	4.27E+02	20.00	6.20E+01
25.10	3.67E+02	25.10	6.31E+01
31.60	3.11E+02	31.60	6.14E+01
39.80	2.62E+02	39.80	5.74E+01
50.10	2.19E+02	50.10	5.16E+01
63.10	1.80E+02	63.10	4.45E+01
79.40	1.44E+02	79.40	3.67E+01
100.00	1.10E+02	100.00	2.87E+01
126.00	7.93E+01	126.00	2.09E+01
158.00	5.33E+01	158.00	1.41E+01
200.00	3.36E+01	200.00	8.83E+00
251.00	1.97E+01	251.00	5.05E+00
316.00	1.06E+01	316.00	2.64E+00
398.00	5.22E+00	398.00	1.25E+00

Differential Fluxes from Solar Proton Events
100 mils Aluminum Shielding, CREME96

Note: Spectra were cut off at E =1 MeV and E=1000 MeV
Values Do Not Include Design Margins

Energy MeV	Proton Flux #/cm²/s Average Over Peak	Proton Flux #/cm²/s Average Over Worst Day	Proton Flux #/cm²/s Average Over Worst Week
1.00	1.75E+03	4.62E+02	8.85E+01
2.00	2.68E+03	7.09E+02	1.36E+02
3.02	3.47E+03	9.17E+02	1.76E+02
4.04	4.11E+03	1.09E+03	2.09E+02
5.04	4.62E+03	1.22E+03	2.36E+02
6.03	5.03E+03	1.33E+03	2.58E+02
7.02	5.33E+03	1.41E+03	2.75E+02
8.06	5.56E+03	1.47E+03	2.88E+02
9.00	5.69E+03	1.51E+03	2.96E+02
10.05	5.76E+03	1.53E+03	3.01E+02
14.99	5.41E+03	1.44E+03	2.92E+02
20.03	4.50E+03	1.21E+03	2.52E+02
24.98	3.57E+03	9.65E+02	2.07E+02
30.31	2.73E+03	7.40E+02	1.64E+02
35.27	2.11E+03	5.75E+02	1.31E+02
40.49	1.61E+03	4.42E+02	1.04E+02
50.50	9.91E+02	2.73E+02	6.79E+01
60.43	6.33E+02	1.75E+02	4.58E+01
70.33	4.20E+02	1.17E+02	3.20E+01
79.63	2.94E+02	8.18E+01	2.33E+01
90.17	2.03E+02	5.65E+01	1.68E+01
100.69	1.44E+02	4.01E+01	1.24E+01
150.25	3.84E+01	1.06E+01	3.80E+00
200.77	1.39E+01	3.79E+00	1.50E+00
299.59	3.32E+00	8.62E-01	3.88E-01
400.31	1.16E+00	2.85E-01	1.39E-01
499.23	4.97E-01	1.16E-01	5.96E-02
605.64	2.07E-01	4.64E-02	2.54E-02
704.94	1.10E-01	2.48E-02	1.44E-02
798.17	6.61E-02	1.48E-02	9.03E-03
903.74	3.95E-02	8.88E-03	5.66E-03
995.41	2.65E-02	5.96E-03	3.94E-03

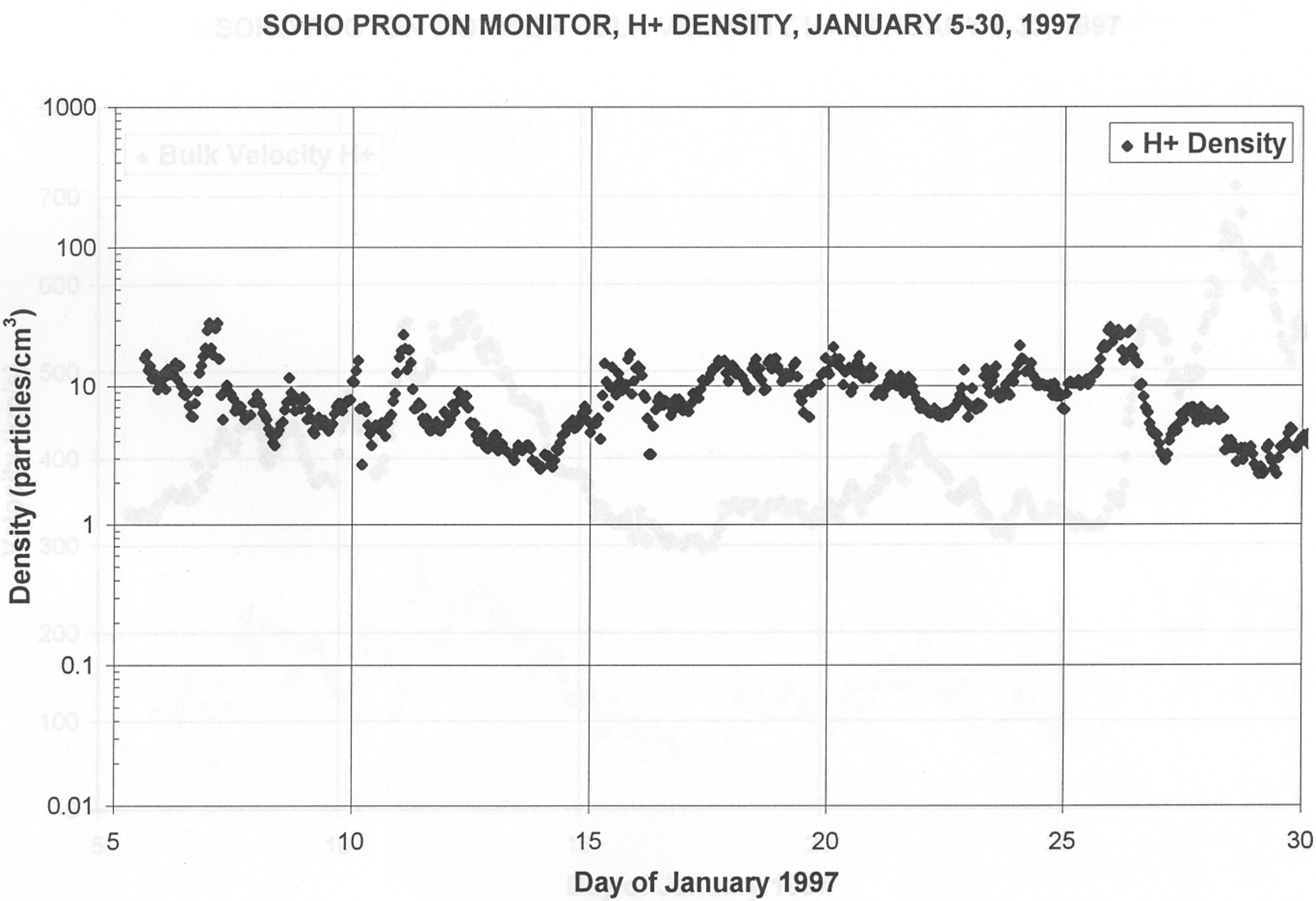
SOHO PROTON MONITOR, H+ DENSITY, JANUARY 5-30, 1997
H+ Density
Density (particles/cm^3)
1000
100
10
1
0.1
0.01
5
10
15
20
25
30
Day of January 1997

Figure 1

SOHO PROTON MONITOR BULK VELOCITY H+ JANUARY 5-30, 1997

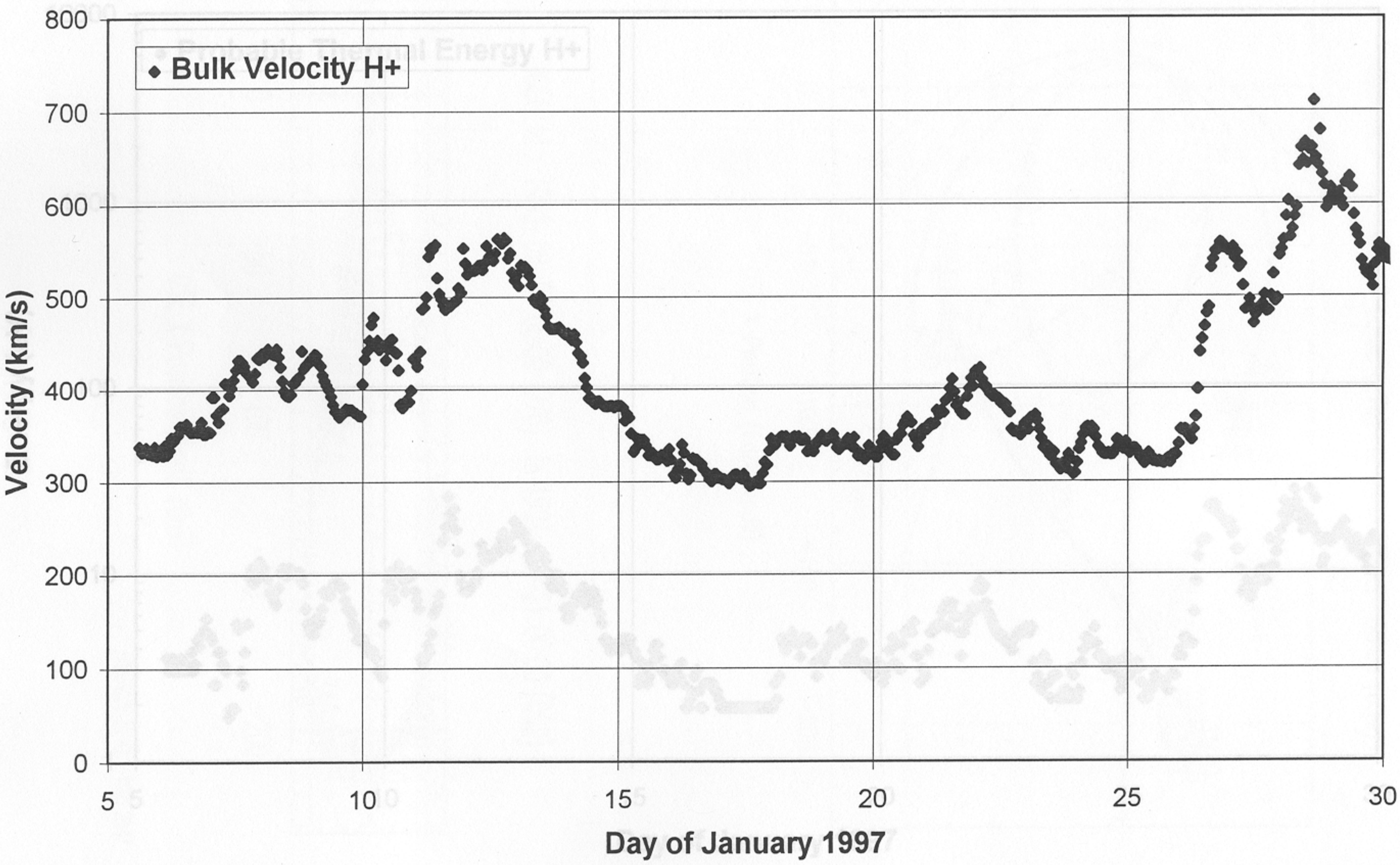

Figure 2

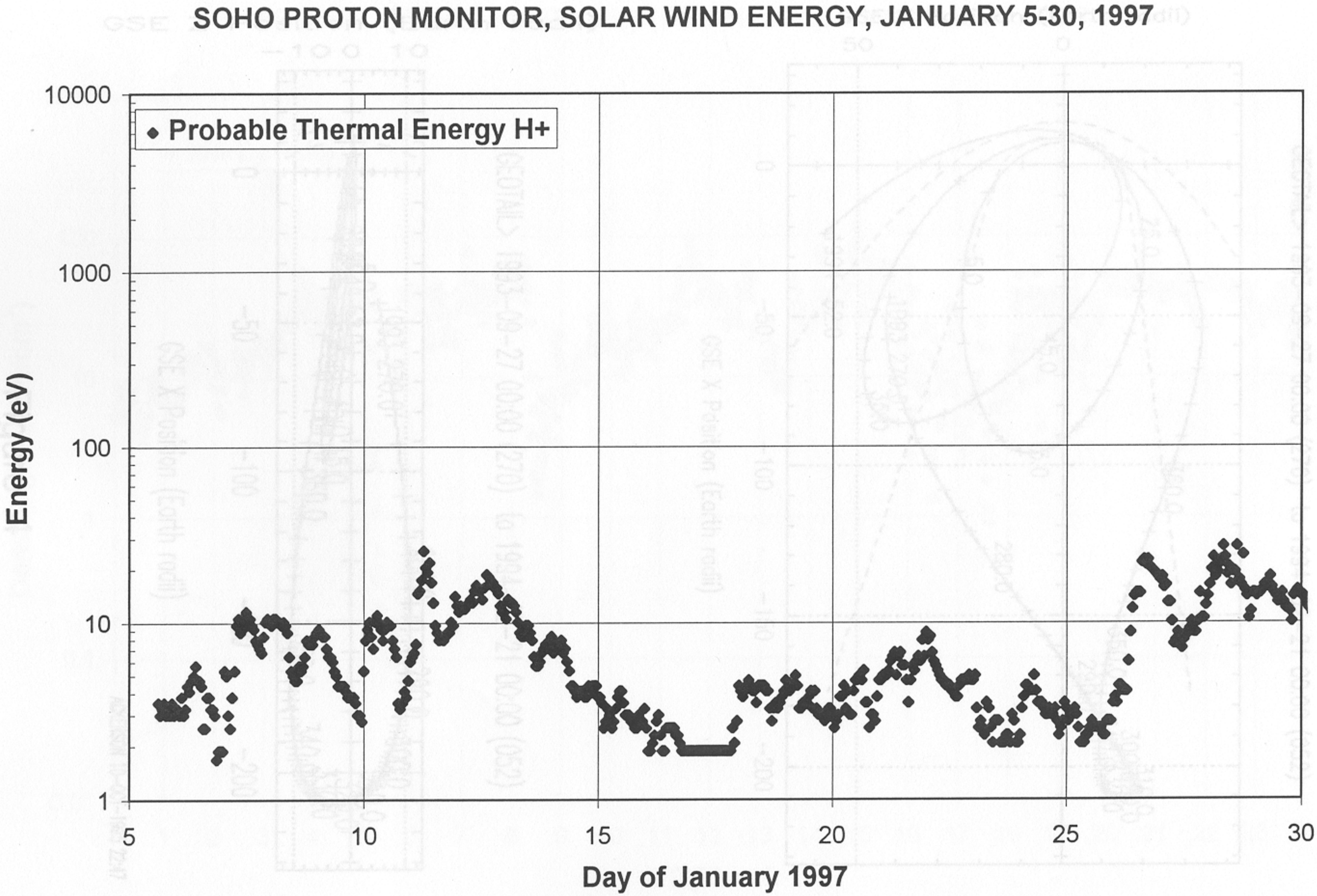
SOHO PROTON MONITOR, SOLAR WIND ENERGY, JANUARY 5-30, 1997
Probable Thermal Energy H+
Energy (eV)
10000
1000
100
10
1
5
10
15
20
25
30
Day of January 1997

Figure 3

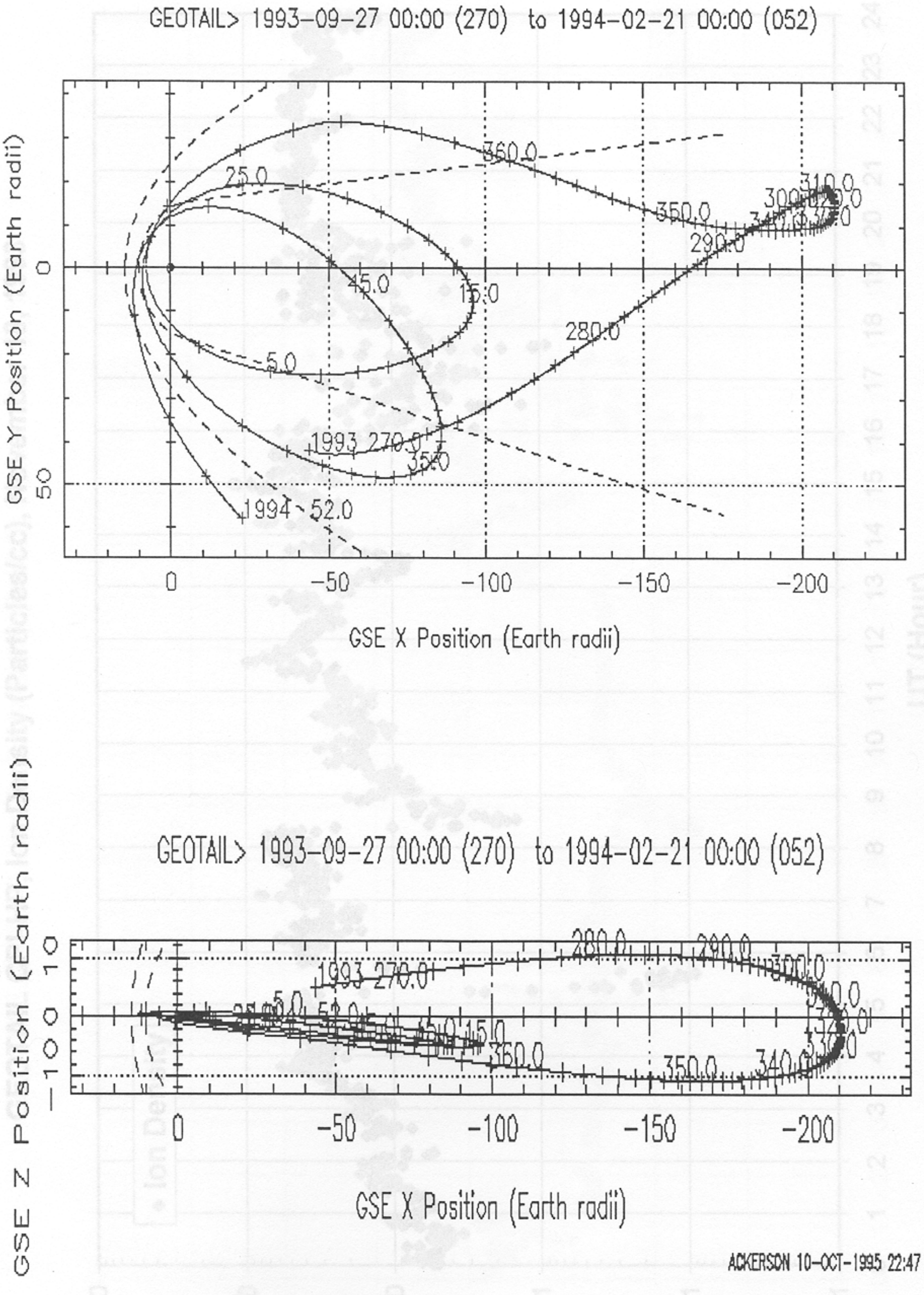
GEOTAIL> 1993-09-27 00:00 (270) to 1994-02-21 00:00 (052)
GSE Y Position (Earth radii)
GSE X Position (Earth radii)
360.0
25.0
350.0
290.0
280.0
45.0
15.0
5.0
1993 270.0
35.0
1994 52.0
GEOTAIL> 1993-09-27 00:00 (270) to 1994-02-21 00:00 (052)
GSE Z Position (Earth radii)
GSE X Position (Earth radii)
280.0
290.0
1993 270.0
300.0
360.0
350.0
340.0
ACKERSON 10-OCT-1995 22:47

Figure 4

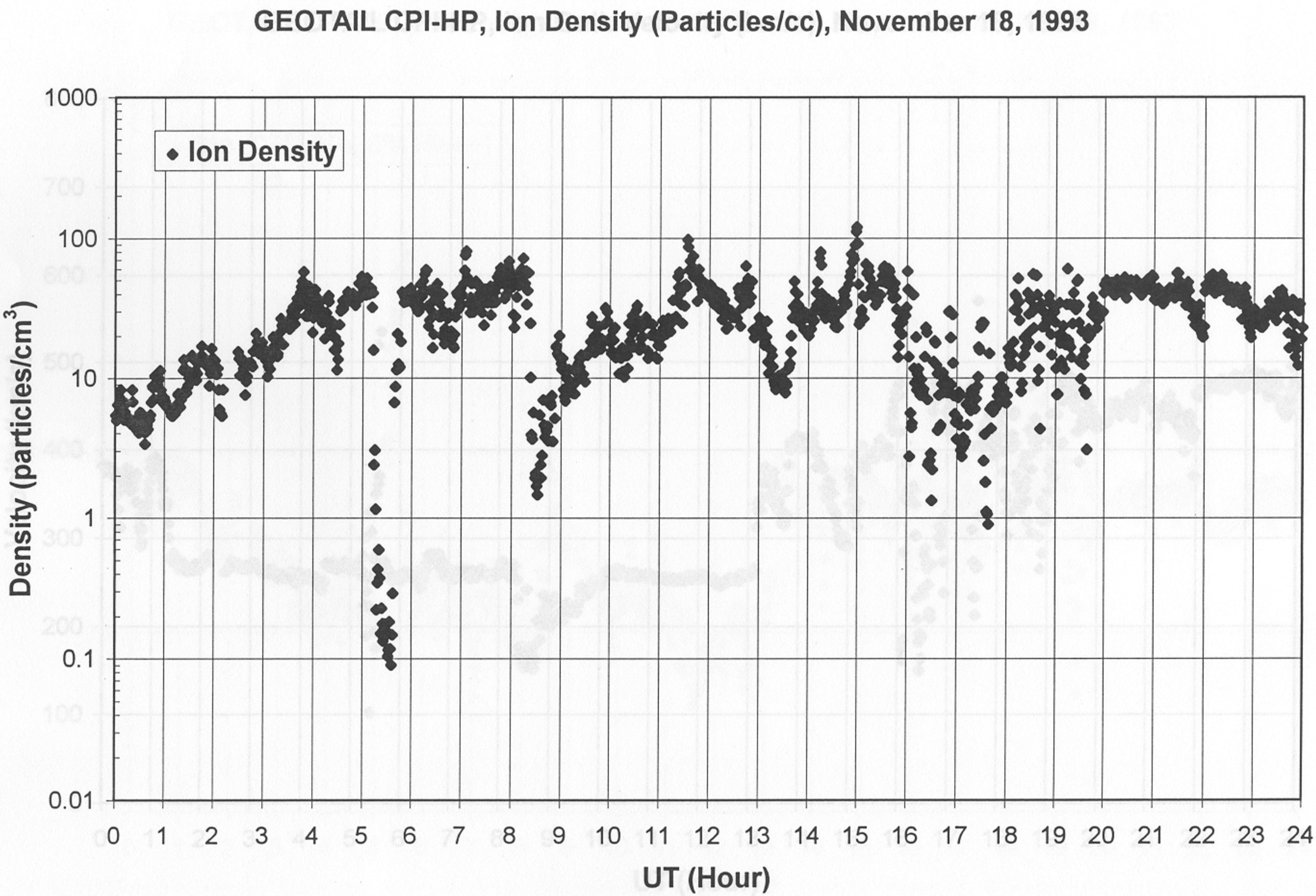
GEOTAIL CPI-HP, Ion Density (Particles/cc), November 18, 1993
Ion Density
Density (particles/cm^3)
1000
100
10
1
0.1
0.01
0
1
2
3
4
5
6
7
8
9
10
11
12
13
14
15
16
17
18
19
20
21
22
23
24
UT (Hour)

Figure 5

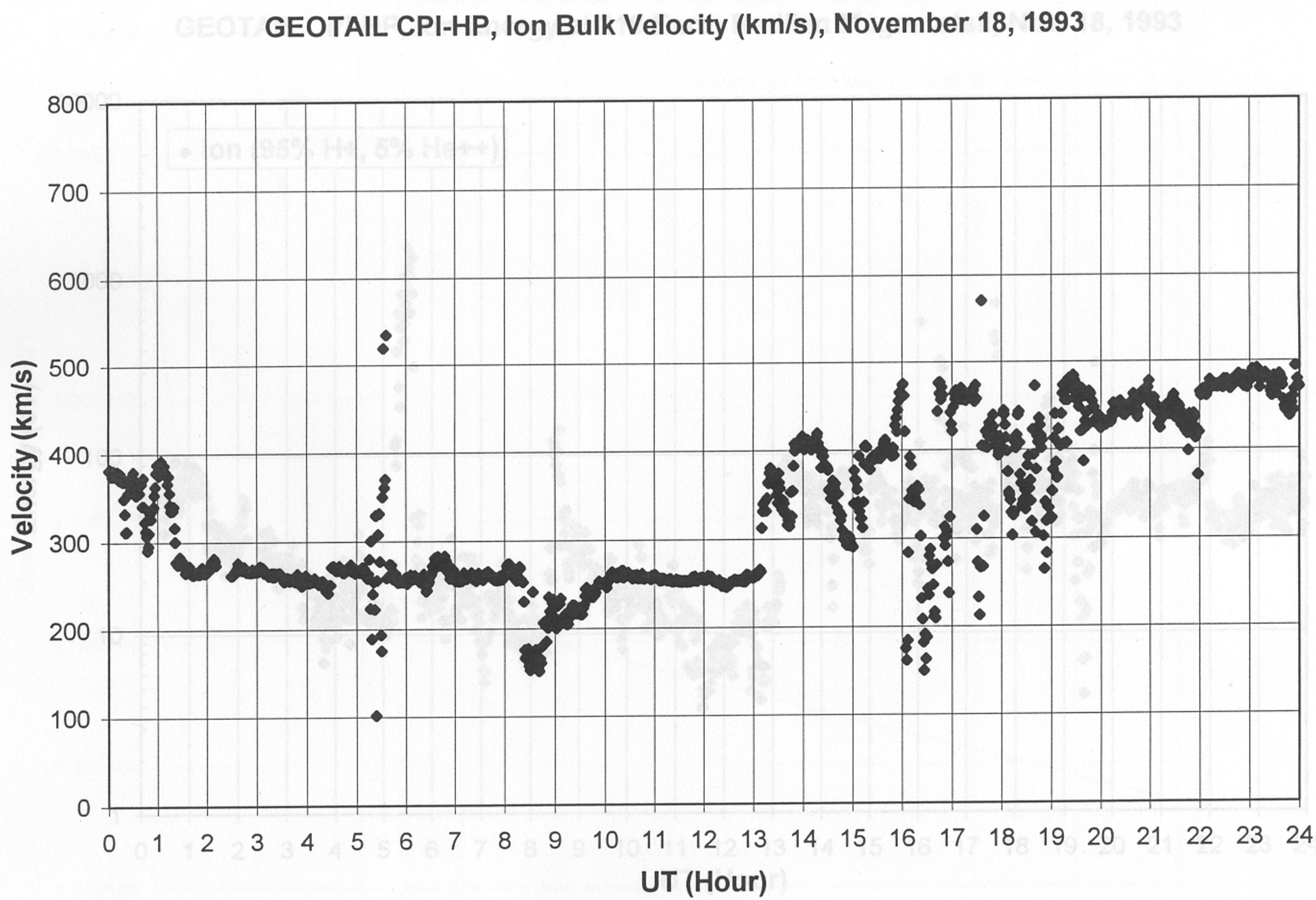
GEOTAIL CPI-HP, Ion Bulk Velocity (km/s), November 18, 1993
Velocity (km/s)
0
100
200
300
400
500
600
700
800
UT (Hour)
0 1 2 3 4 5 6 7 8 9 10 11 12 13 14 15 16 17 18 19 20 21 22 23 24

Figure 6

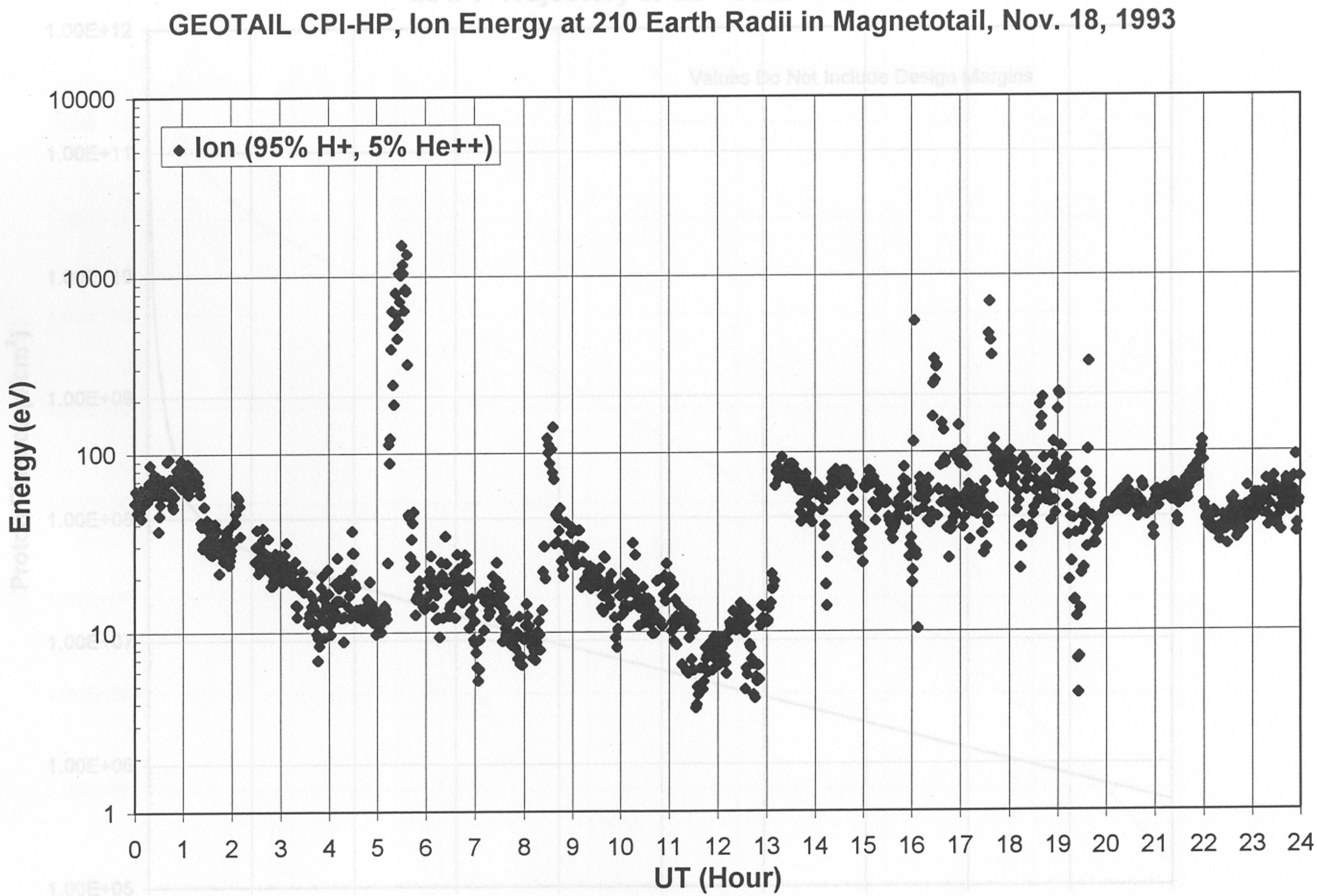
GEOTAIL CPI-HP, Ion Energy at 210 Earth Radii in Magnetotail, Nov. 18, 1993
Ion (95% H+, 5% He++)
Energy (eV)
10000
1000
100
10
1
0 1 2 3 4 5 6 7 8 9 10 11 12 13 14 15 16 17 18 19 20 21 22 23 24
UT (Hour)

Figure 7

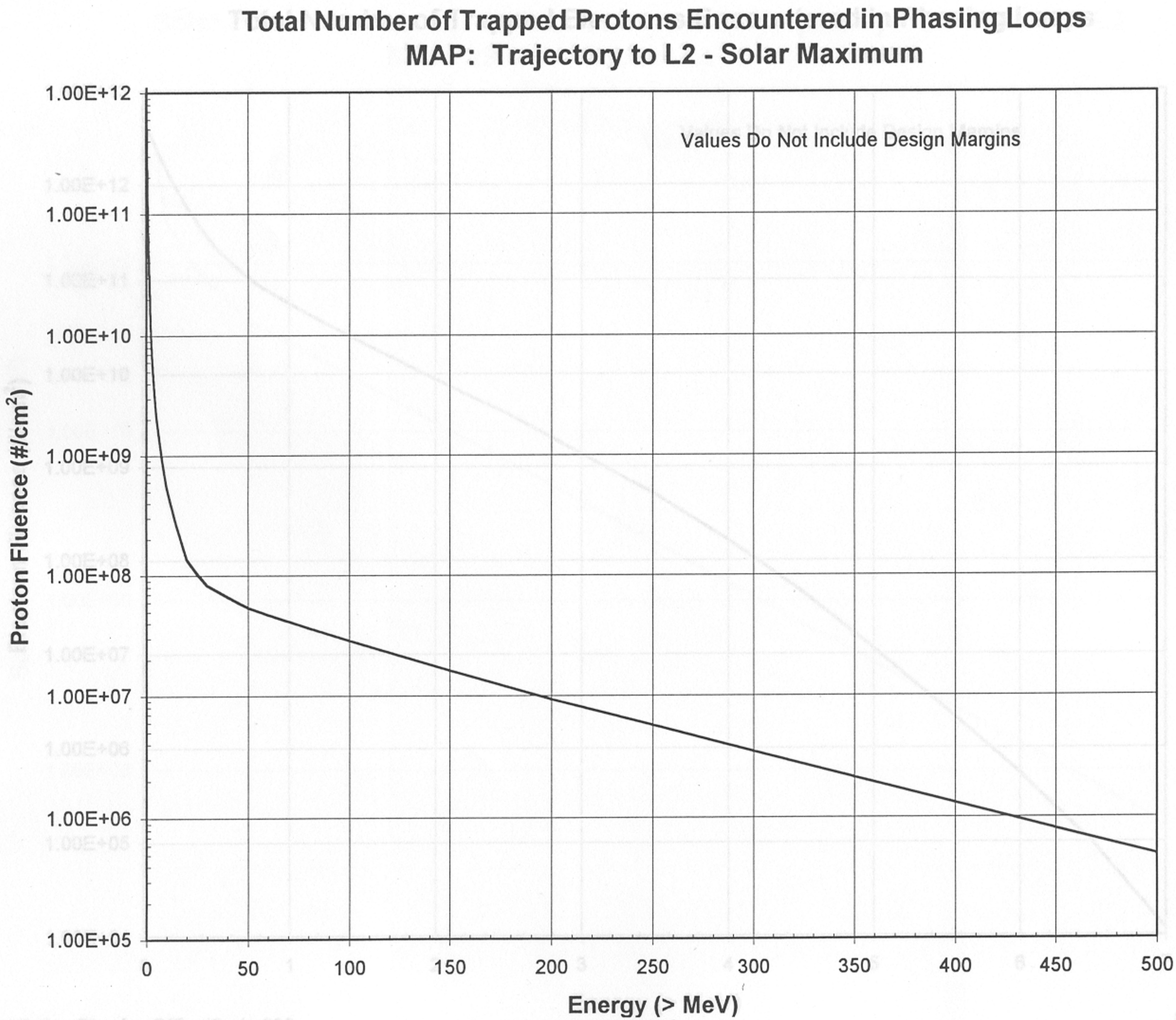

Radiation Physics Office/Code 900

NASA/GSFC-1996

Figure 8

Total Number of Trapped Electrons Encountered in Phasing Loops
MAP: Trajectory to L2 - Solar Maximum

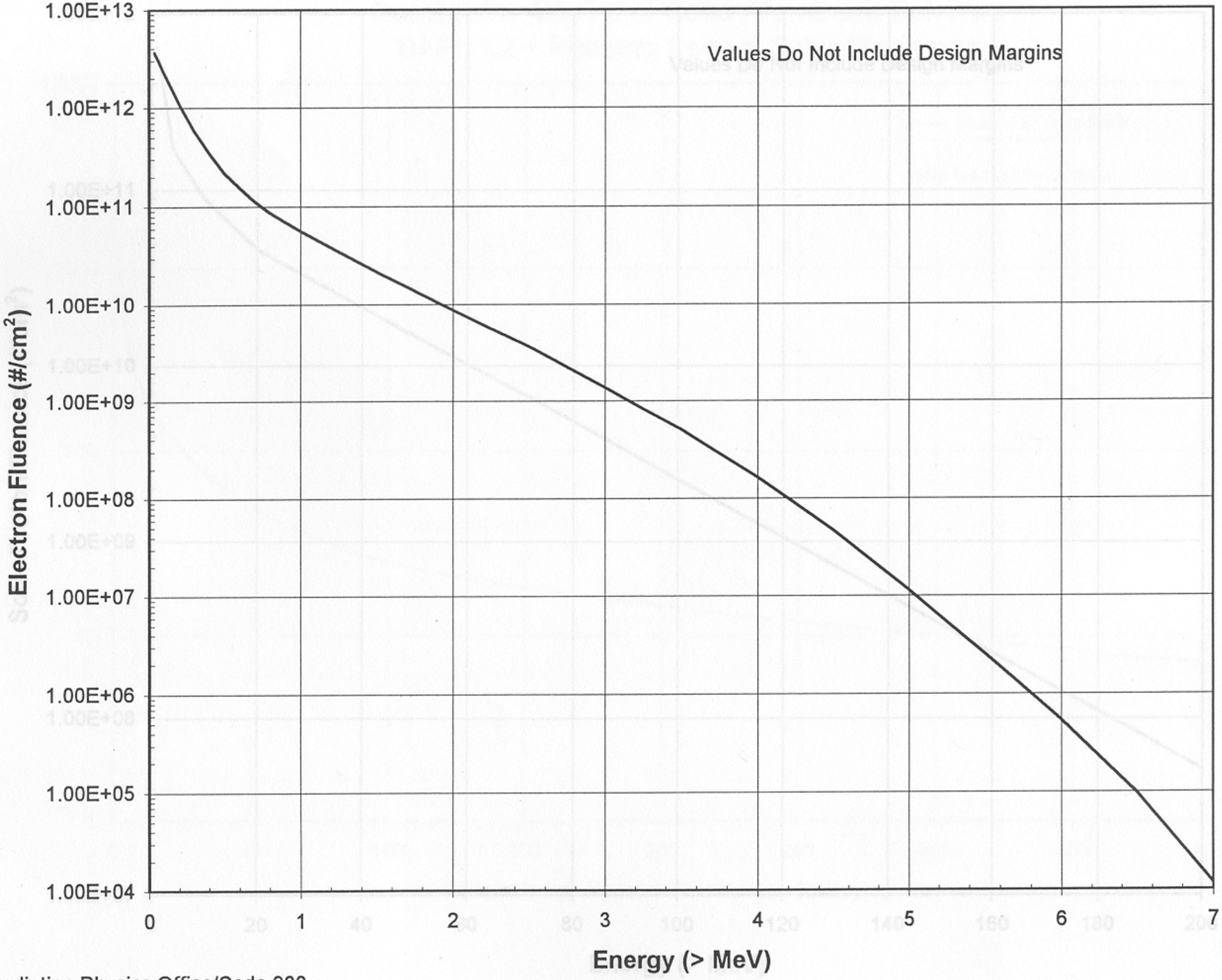

Radiation Physics Office/Code 900

NASA/GSFC-1996

Figure 9

Solar Proton Fluence for 27 Months - Transfer Trajectory + 24 Months at L2
MAP: 99% Confidence Level - 4 Events

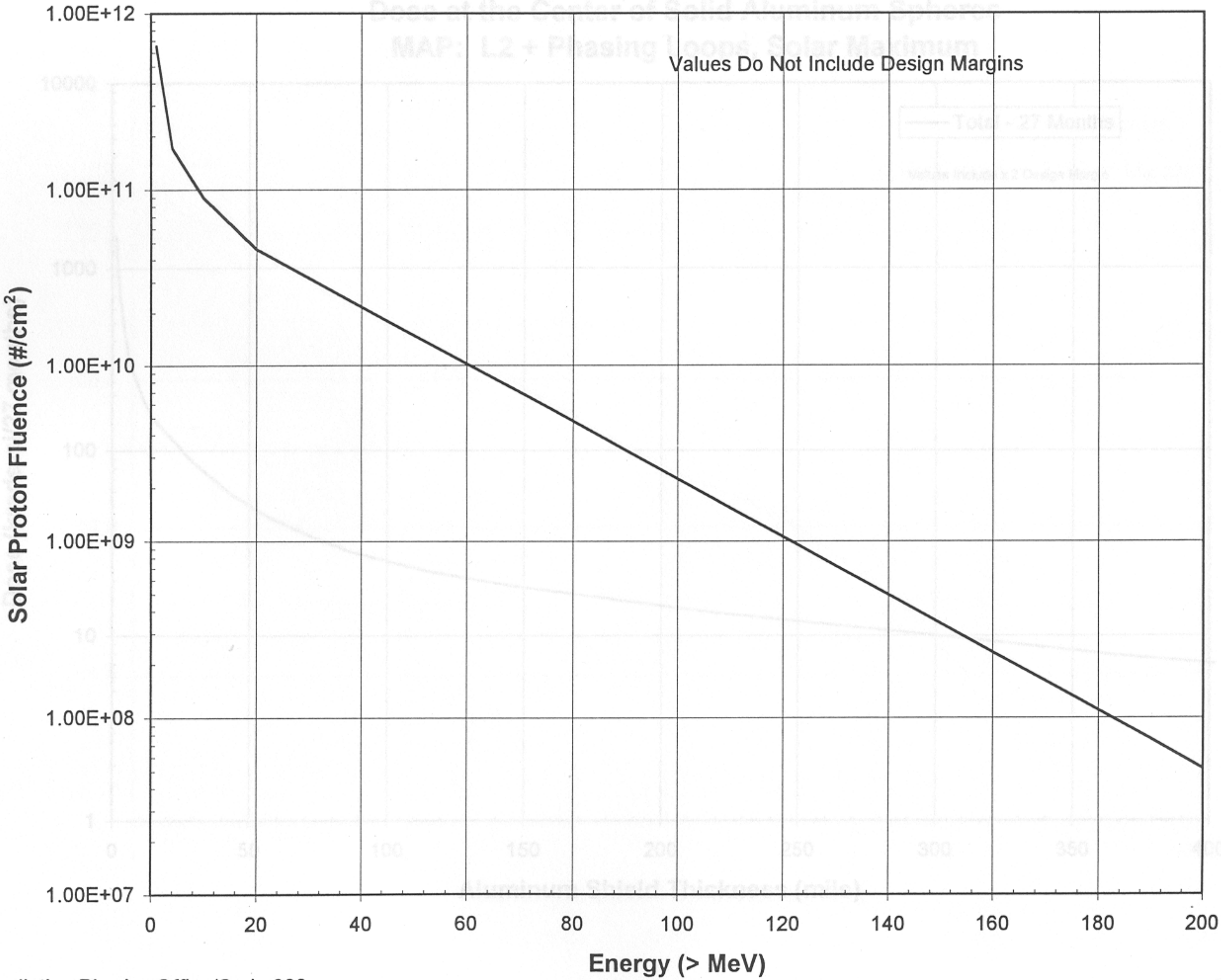

Radiation Physics Office/Code 900

NASA/GSFC-1996

Figure 10

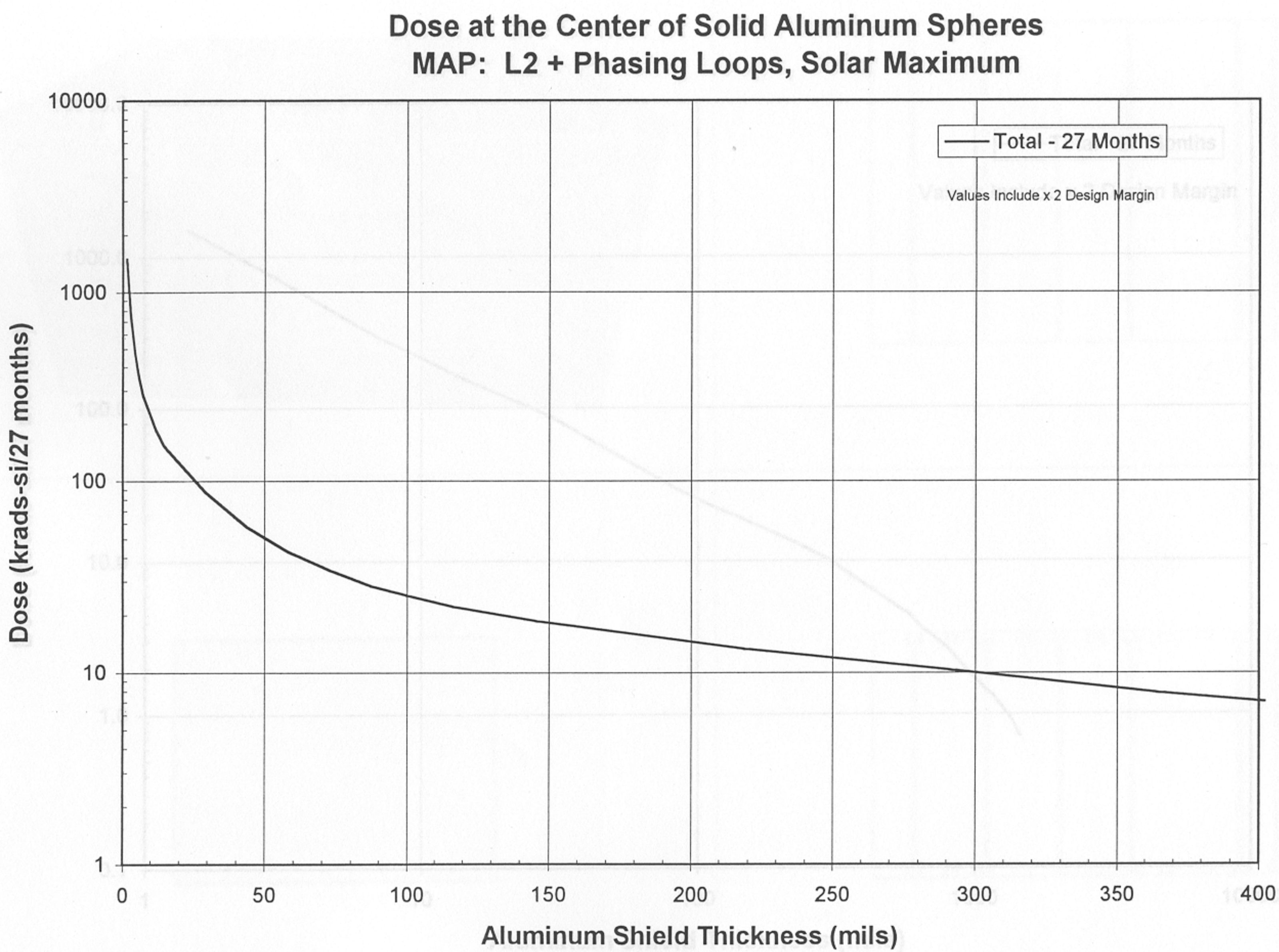
Dose at the Center of Solid Aluminum Spheres
MAP: L2 + Phasing Loops, Solar Maximum
Dose (krads-si/27 months)
10000
1000
100
10
1
0
50
100
150
200
250
300
350
400
Aluminum Shield Thickness (mils)
Total - 27 Months
Values Include x 2 Design Margin

Figure 11

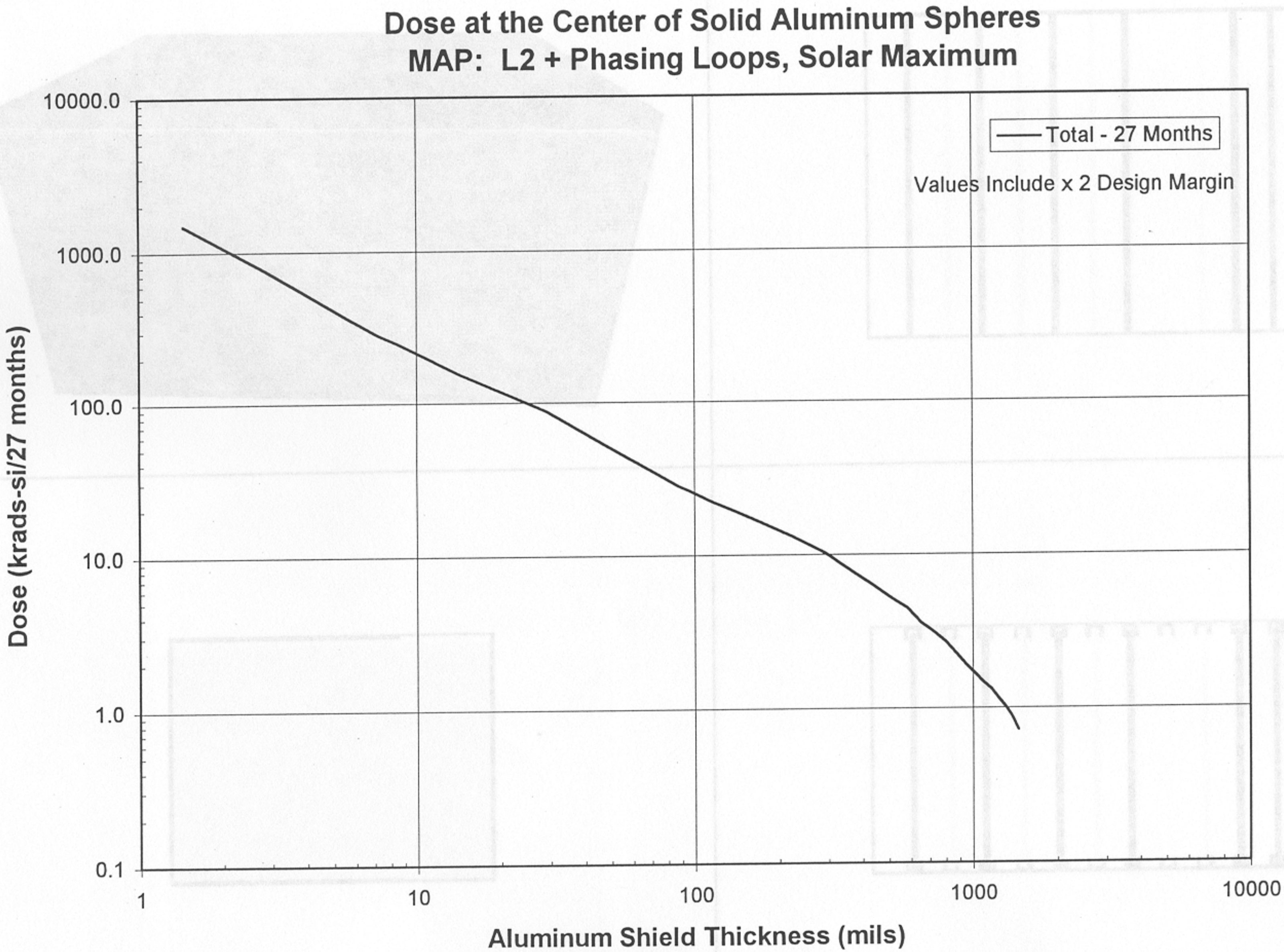

Radiation Physics Office/Code 900

Figure 12

NASA/GSFC-1996

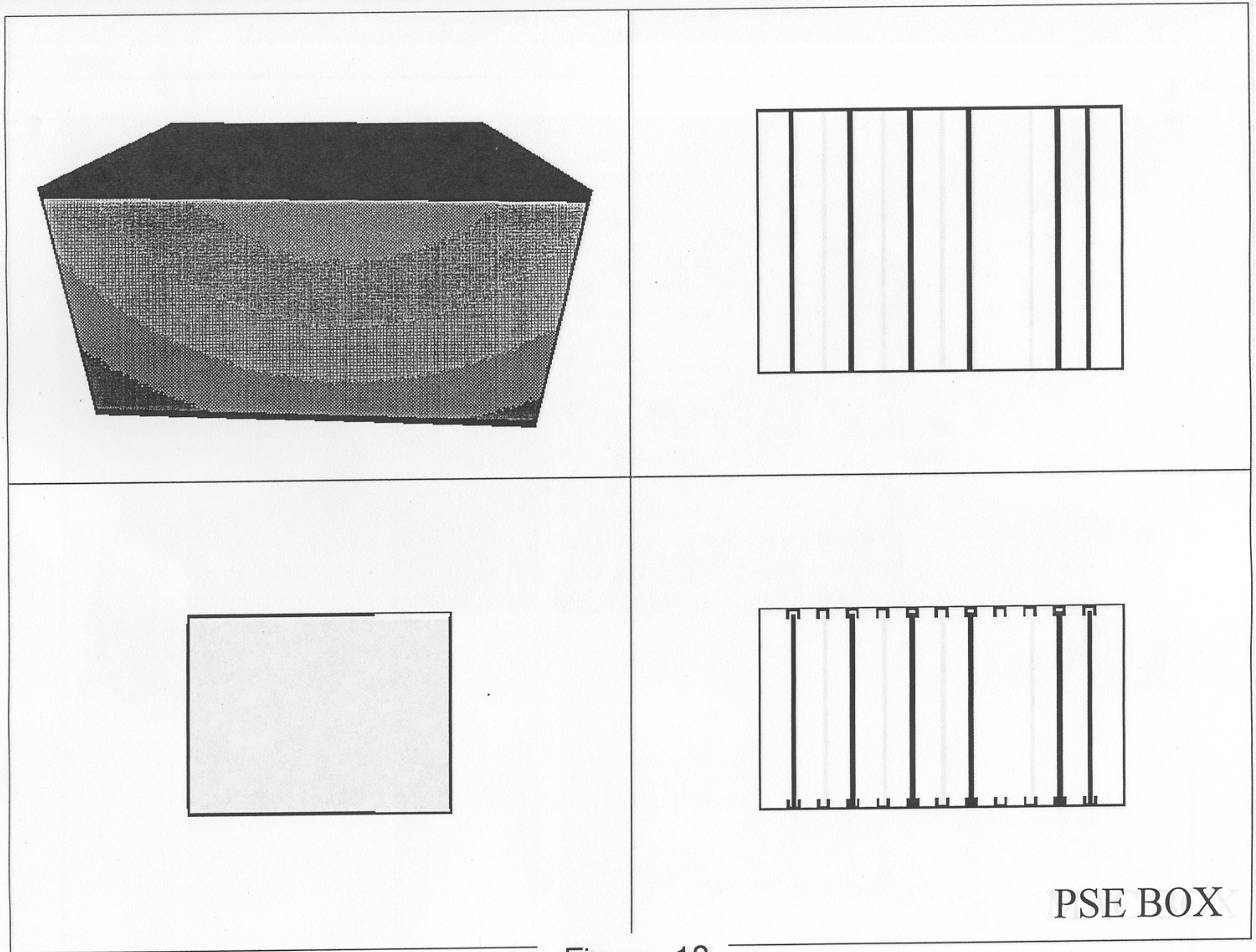

Figure 13

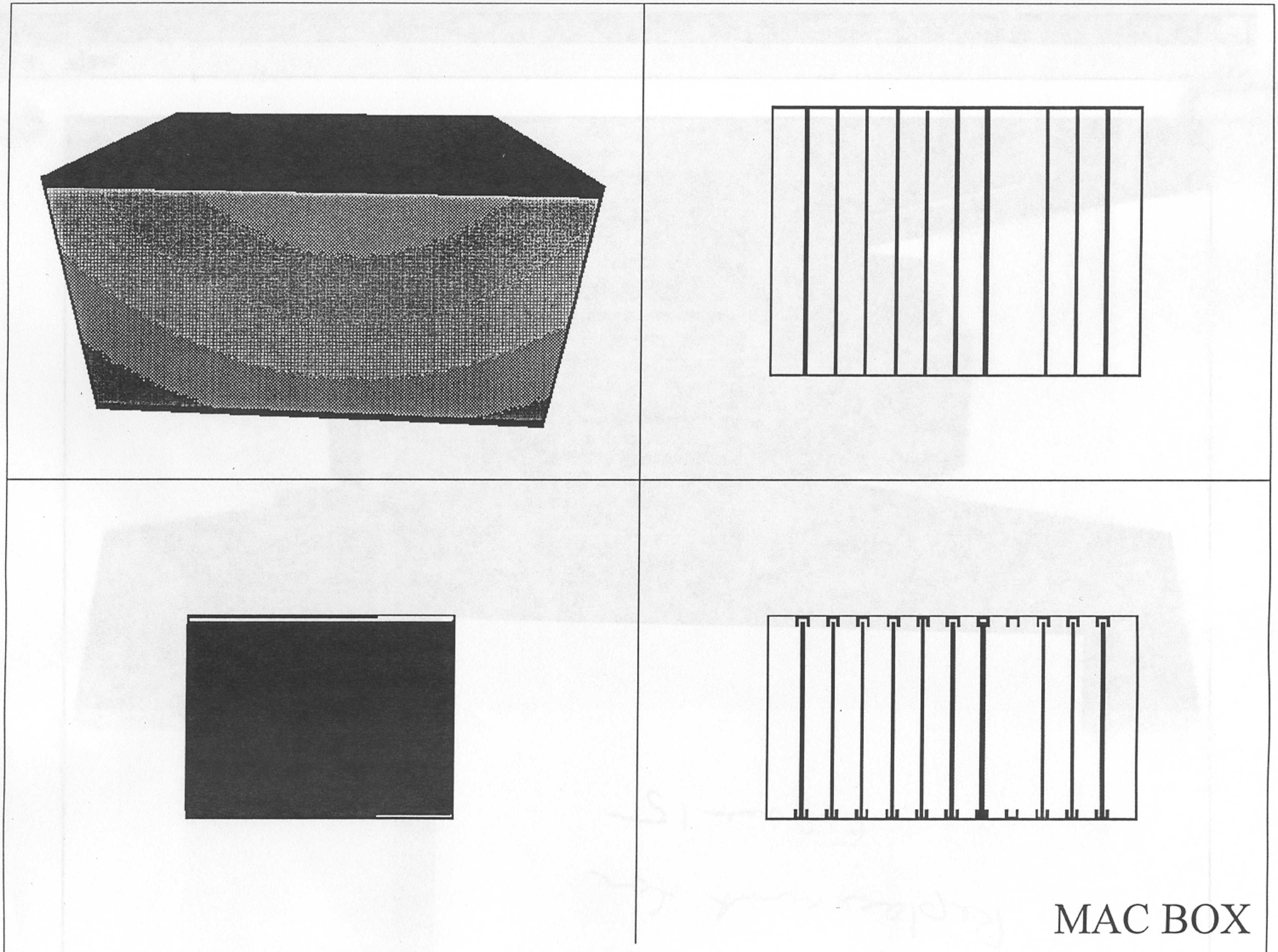

Figure 14

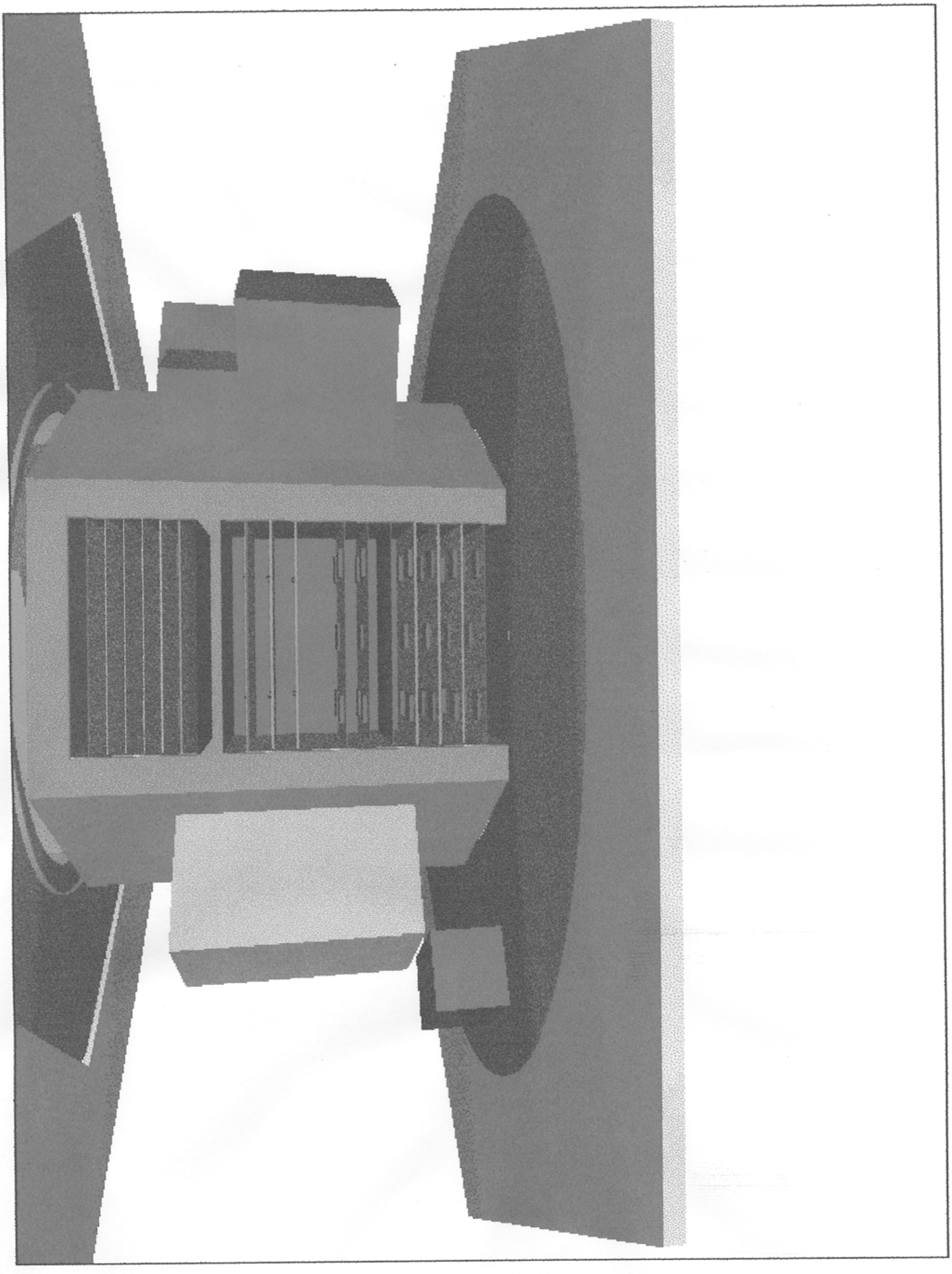

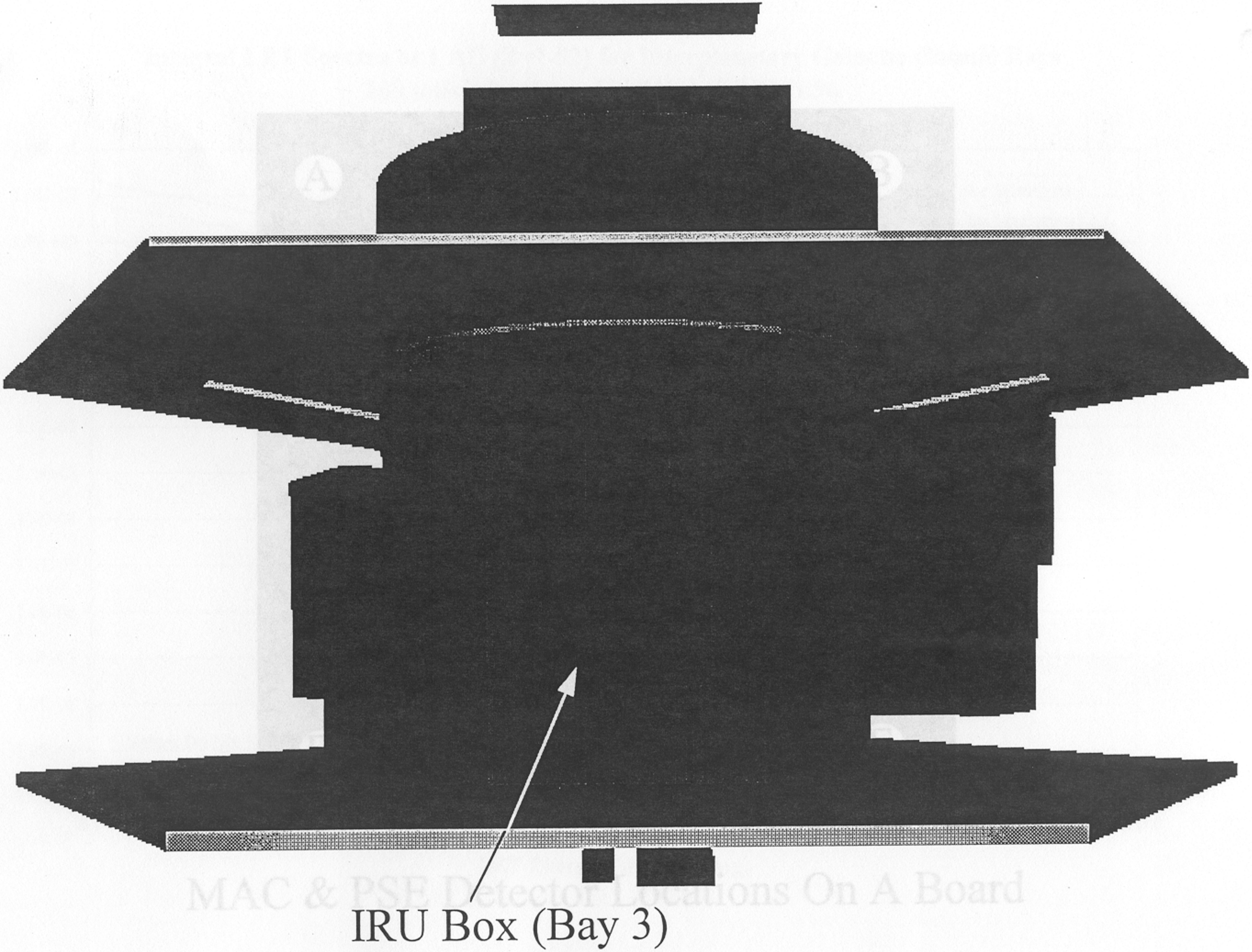

Figure 16

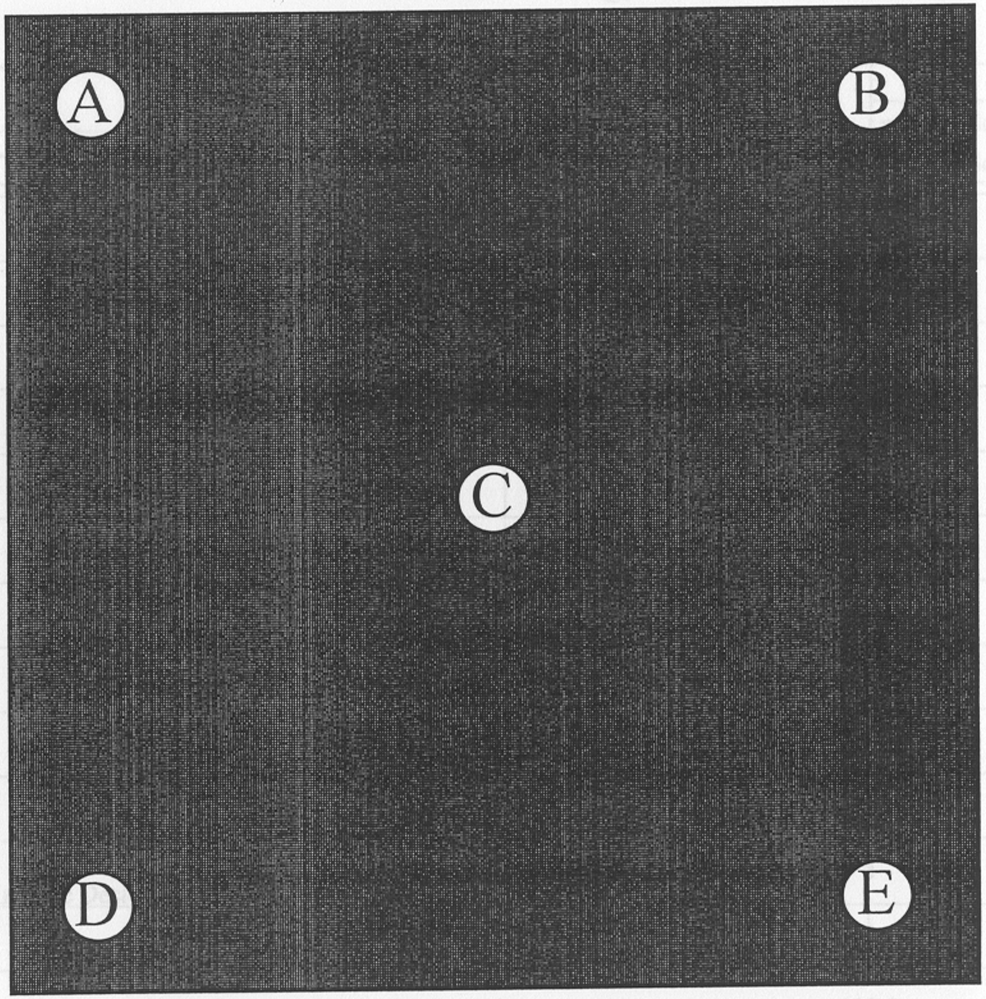

MAC & PSE Detector Locations On A Board

Figure 17

Integral LET Spectra at 1 AU (Z=1-92) for Interplanetary Galactic Cosmic Rays
100 mils Aluminum Shielding, CREME96

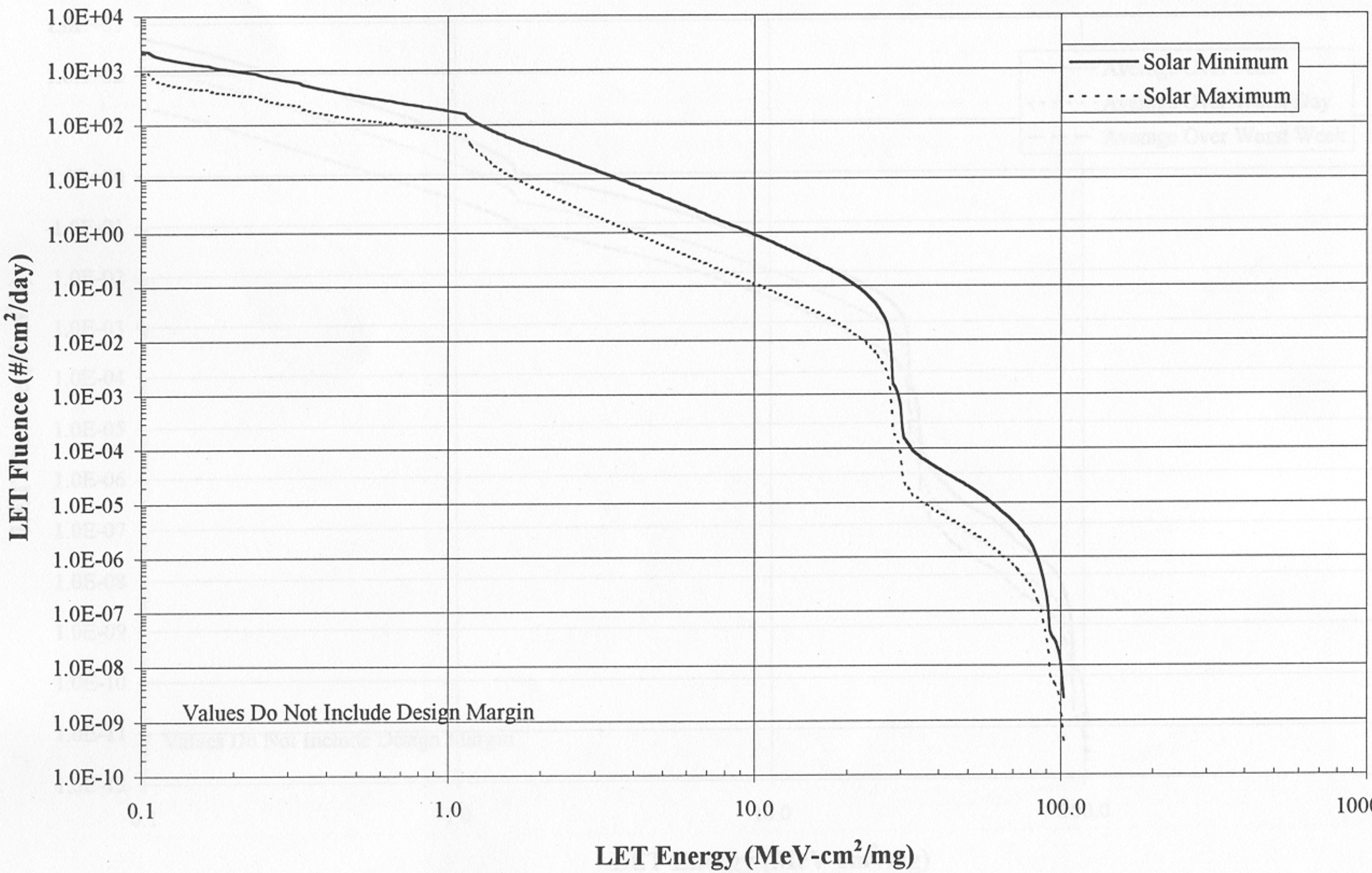

Figure 18

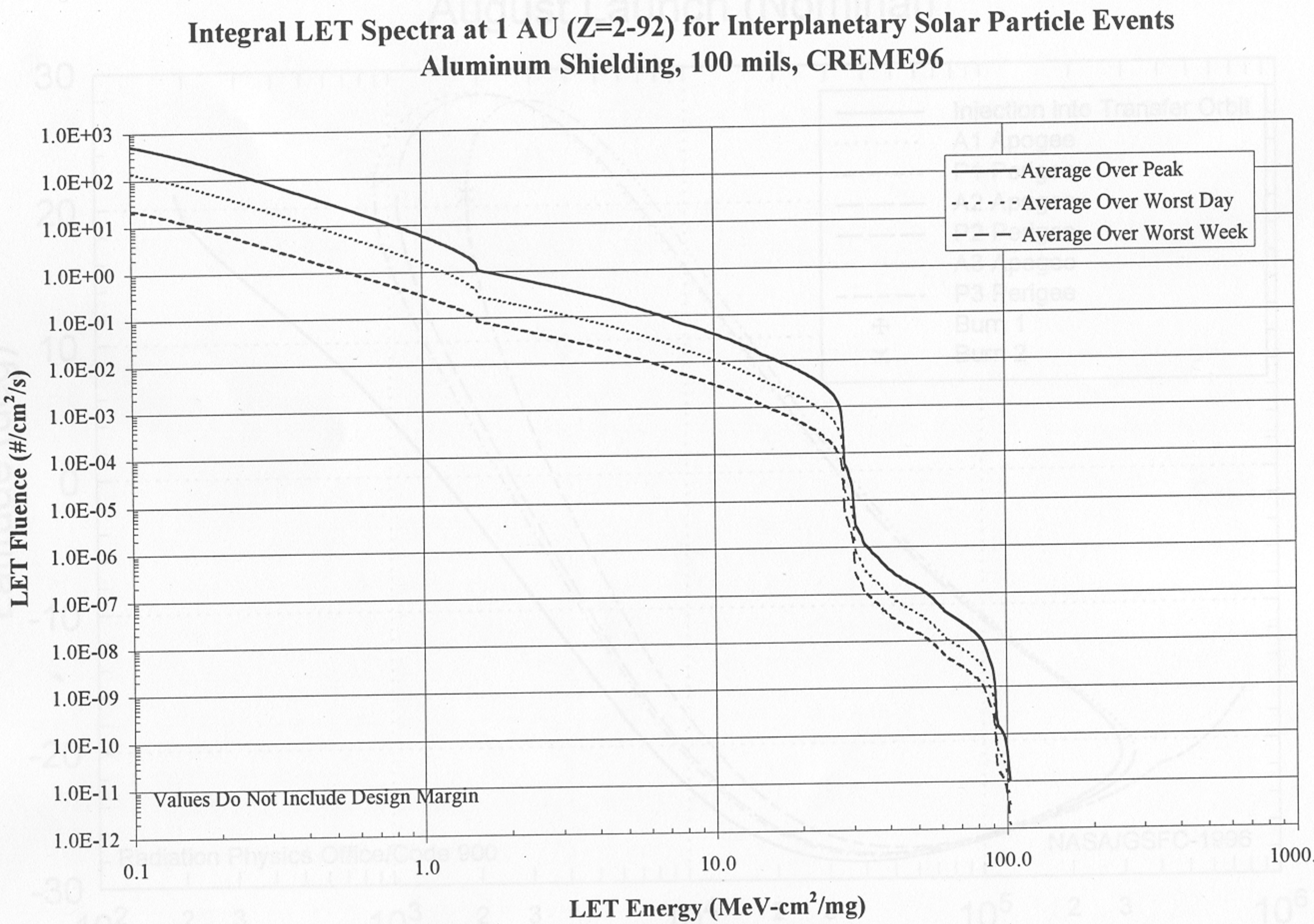

Integral LET Spectra at 1 AU (Z=2-92) for Interplanetary Solar Particle Events
Aluminum Shielding, 100 mils, CREME96
Average Over Peak
Average Over Worst Day
Average Over Worst Week
1.0E+03
1.0E+02
1.0E+01
1.0E+00
1.0E-01
1.0E-02
1.0E-03
1.0E-04
1.0E-05
1.0E-06
1.0E-07
1.0E-08
1.0E-09
1.0E-10
1.0E-11
1.0E-12
LET Fluence (#/cm²/s)
Values Do Not Include Design Margin
0.1
1.0
10.0
100.0
1000.0
LET Energy (MeV-cm²/mg)

Figure 19

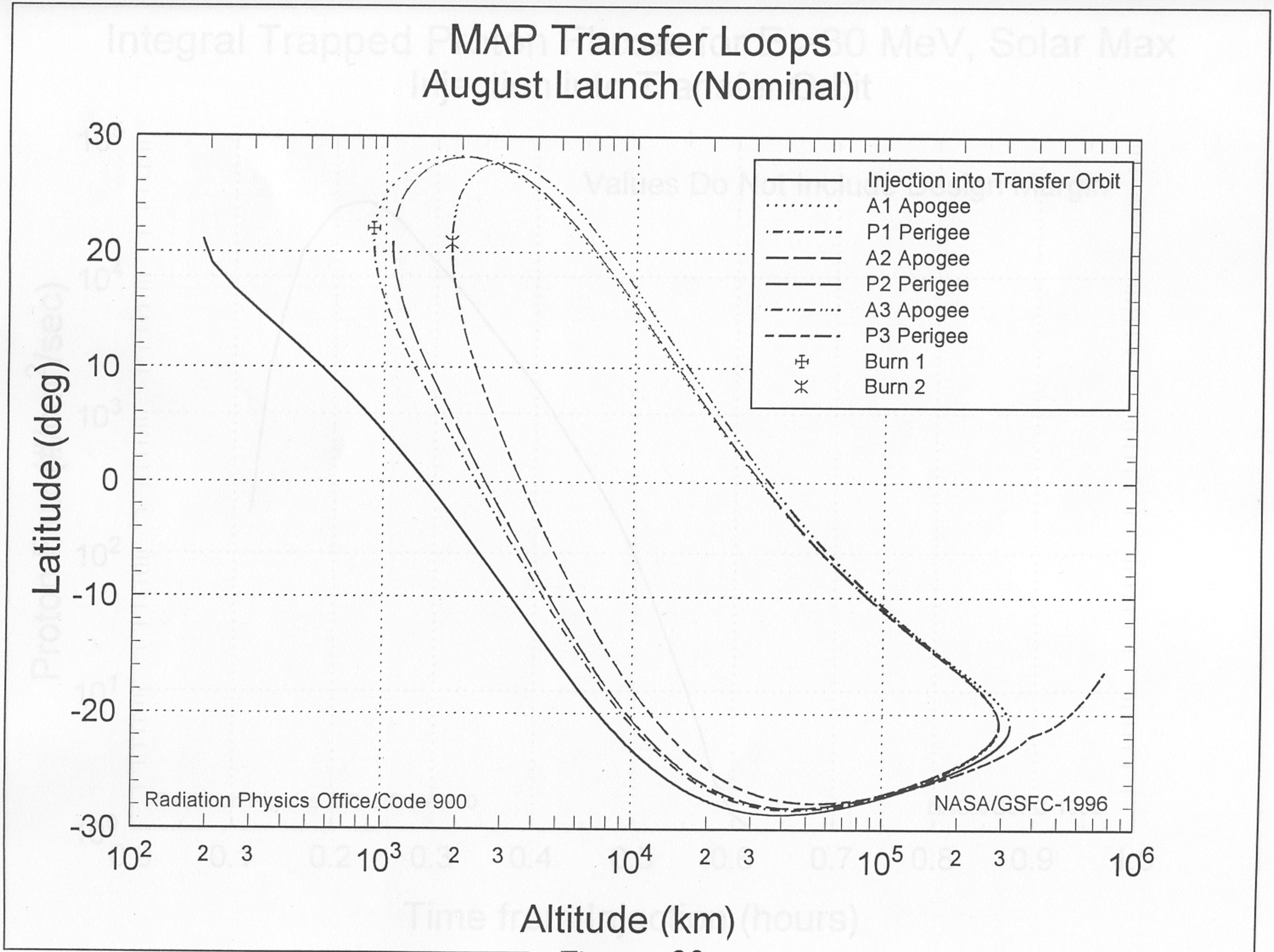

MAP Transfer Loops
August Launch (Nominal)
Latitude (deg)
30
20
10
0
-10
-20
-30
Altitude (km)
10^2
2
3
10^3
2
3
10^4
2
3
10^5
2
3
10^6
Injection into Transfer Orbit
A1 Apogee
P1 Perigee
A2 Apogee
P2 Perigee
A3 Apogee
P3 Perigee
Burn 1
Burn 2
Radiation Physics Office/Code 900
NASA/GSFC-1996

Figure 20

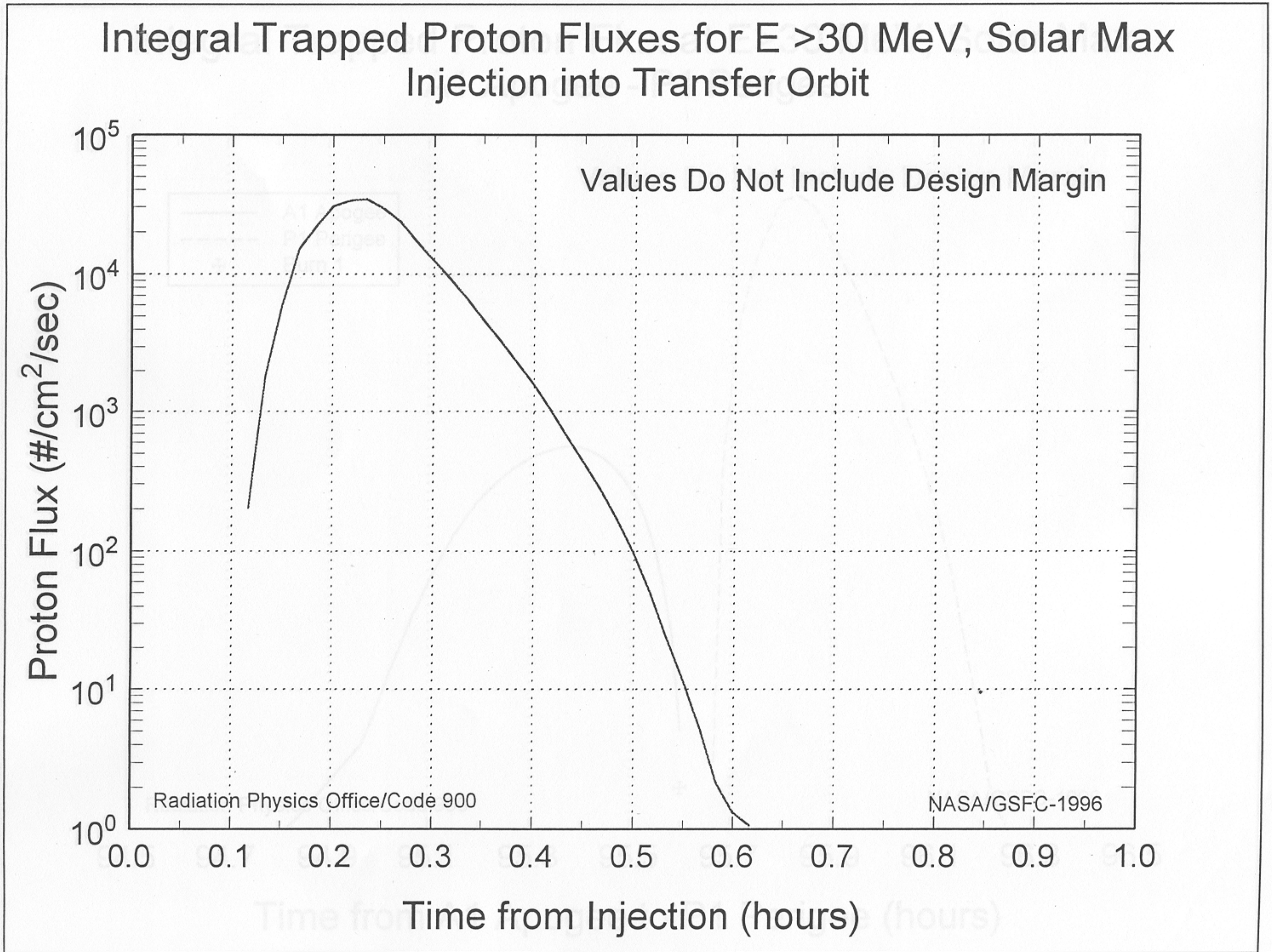

Integral Trapped Proton Fluxes for E >30 MeV, Solar Max
Injection into Transfer Orbit
Values Do Not Include Design Margin
Proton Flux (#/cm²/sec)
10^5
10^4
10^3
10^2
10^1
10^0
0.0
0.1
0.2
0.3
0.4
0.5
0.6
0.7
0.8
0.9
1.0
Time from Injection (hours)
Radiation Physics Office/Code 900
NASA/GSFC-1996

Figure 21

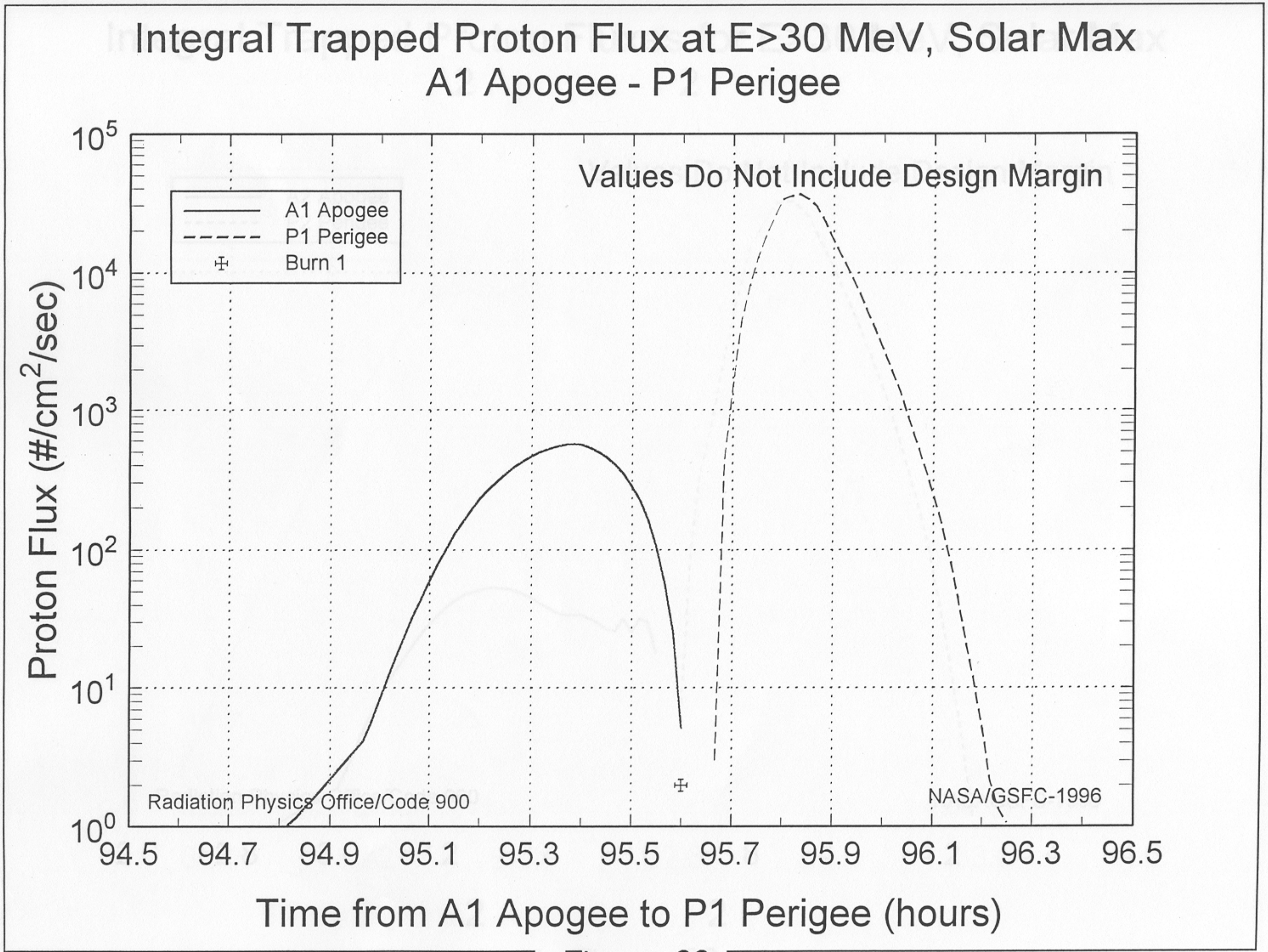

Integral Trapped Proton Flux at E>30 MeV, Solar Max
A1 Apogee - P1 Perigee
Values Do Not Include Design Margin
A1 Apogee
P1 Perigee
Burn 1
Proton Flux (#/cm²/sec)
10^5
10^4
10^3
10^2
10^1
10^0
94.5
94.7
94.9
95.1
95.3
95.5
95.7
95.9
96.1
96.3
96.5
Time from A1 Apogee to P1 Perigee (hours)
Radiation Physics Office/Code 900
NASA/GSFC-1996

Figure 22

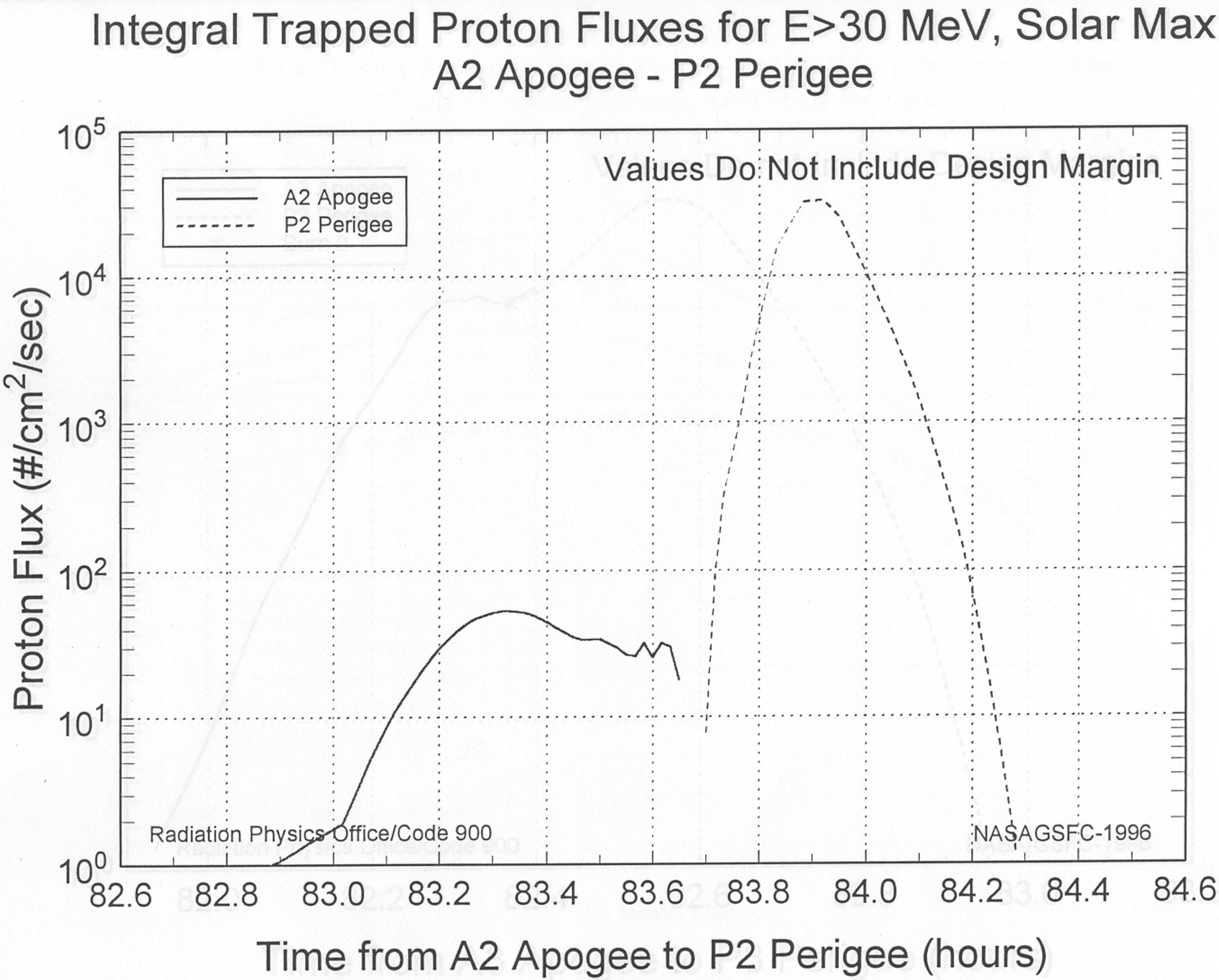

Integral Trapped Proton Fluxes for E>30 MeV, Solar Max
A2 Apogee - P2 Perigee
Values Do Not Include Design Margin
A2 Apogee
P2 Perigee
Proton Flux (#/cm²/sec)
10^5
10^4
10^3
10^2
10^1
10^0
82.6
82.8
83.0
83.2
83.4
83.6
83.8
84.0
84.2
84.4
84.6
Radiation Physics Office/Code 900
NASAGSFC-1996
Time from A2 Apogee to P2 Perigee (hours)

Figure 23

Integral Trapped Proton Fluxes for E>30 MeV, Solar Max
A3 Apogee - P3 Perigee

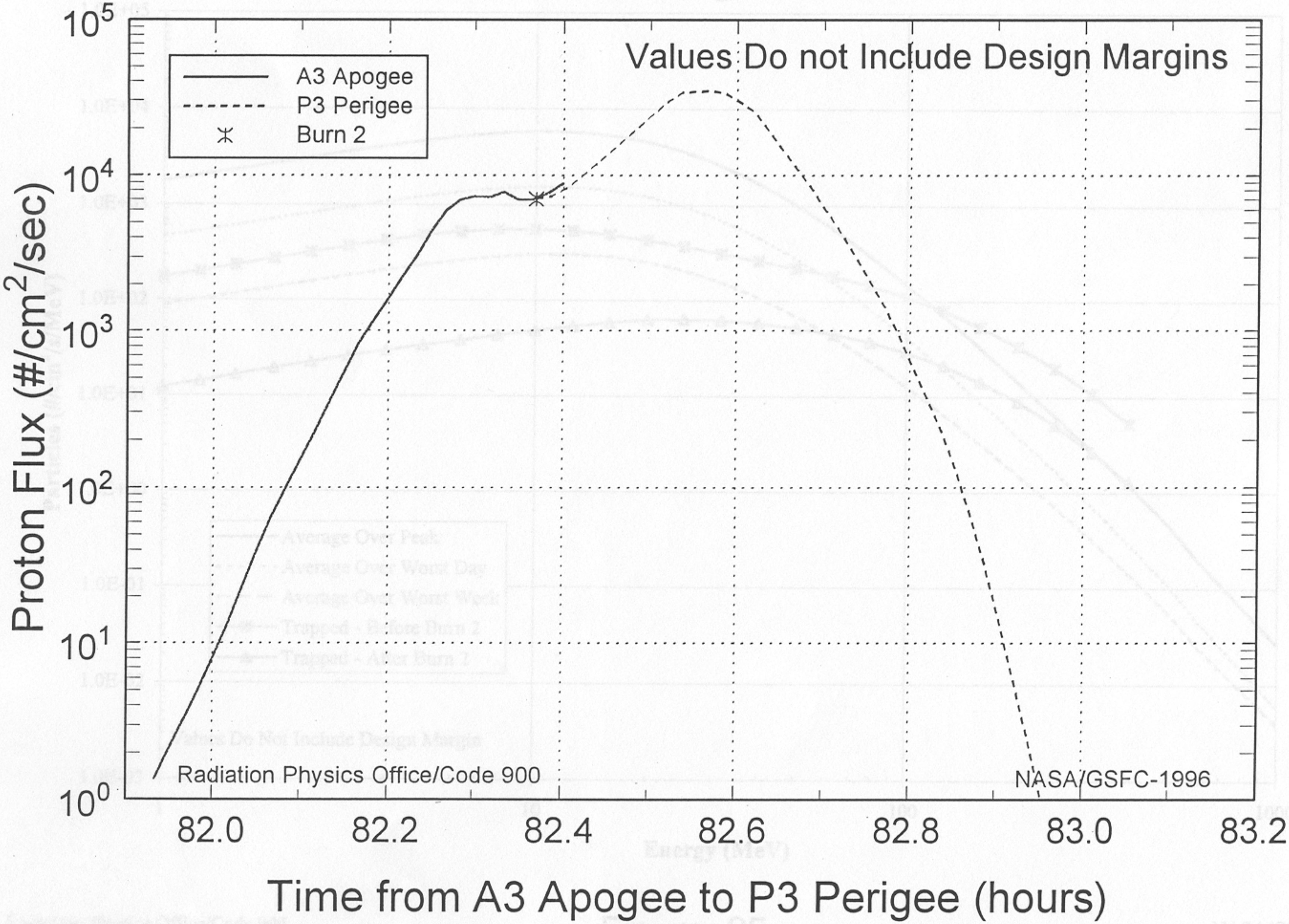

Figure 24

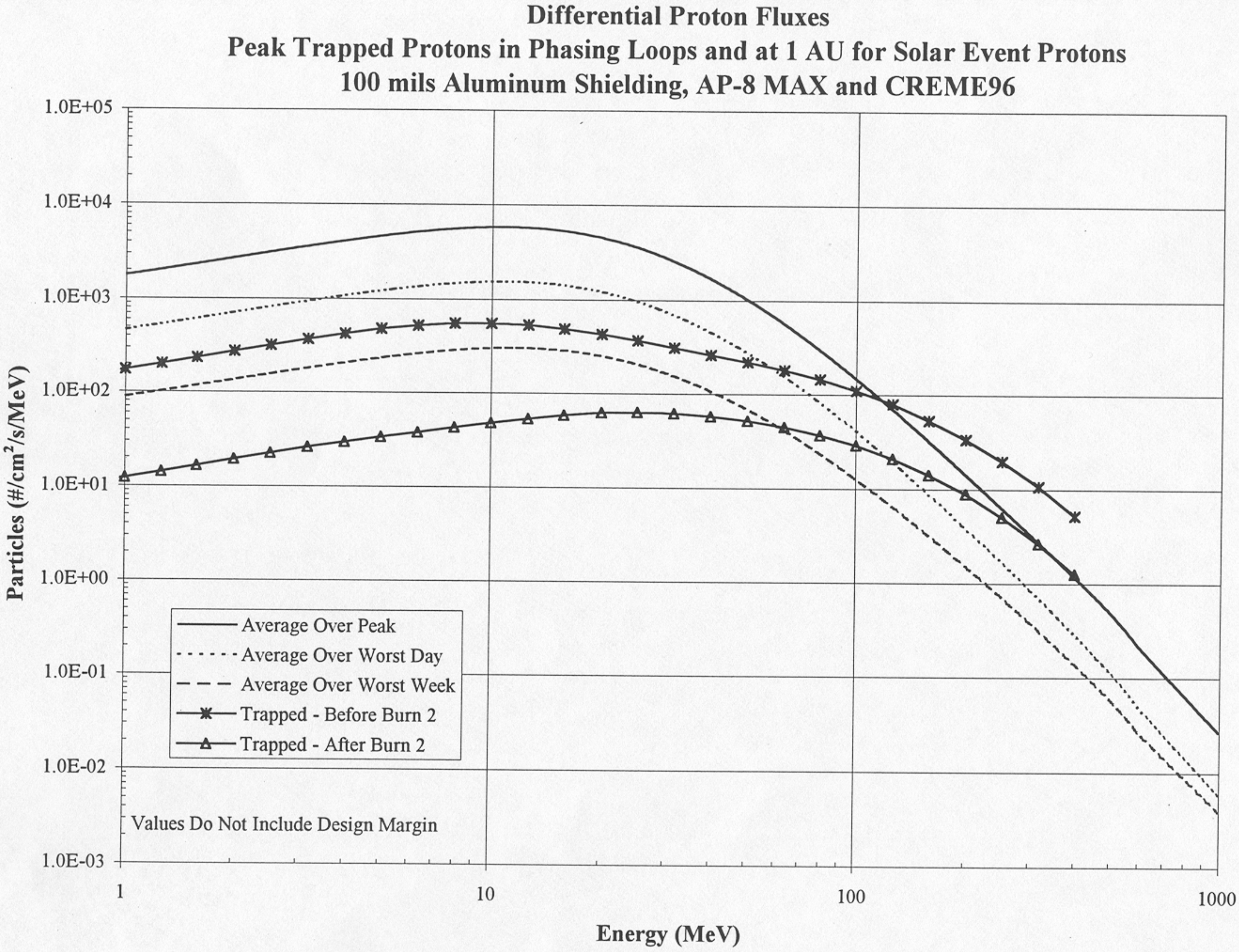

Radiation Physics Office/Code 900

Figure 25

NASA/GSFC-1997